

Sensor and Simulation Notes
Note 142
January 1972

CLASSIFIED
FOR PUBLIC RELEASE
PL/PA 16 DEC 96

The Effects of Constructing a Conical Antenna
Above a Ground Plane Out of a Number of Thin Wires

by
Lt. Daniel F. Higgins

Abstract

Due to mechanical constraints many antenna structures used in EMP simulation are built of sparse wire arrays rather than solid sheets of a conductor. The effects of a specific configuration of wire conductors approximating a conical antenna above a perfectly conducting ground are considered here. The configuration studied consists of N thin wires spaced at equal angles around the surface of a cone, the axis of which is perpendicular to a ground plane. An equivalent solid cone is defined and compared to the sparse N -wire cone. Also, paths for constant impedance are calculated.

Acknowledgement

I wish to thank Mr. Terry L. Brown of the Dikewood Corporation and Sgt. Robert N. Marks of AFWL for the computer programming involved in preparing the graphs attached to this note. I would also like to thank Dr. Carl E. Baum for his interest and advice in the preparation of this work.

PL 96-0957

I. Introduction

The problem of TEM propagation from a conical antenna or wave guide has already been considered in several places.^{1,2,3} The method of solution basically involves a transformation of coordinates from a conical geometry into an equivalent cylindrical system where transmission line theory is applied. Previous work, however, has considered the conical conductors to be solid sheets. In actual practice such solid sheets are often approximated by rather sparse structures made of various arrays of wires so as to ease construction, minimize wind loading, and decrease the total weight of the structure. The purpose of this note is to consider the effects of replacing the solid conical sheets by a number of thin wires running along the conical surfaces. The potentials due to these sparse cylindrical structures are calculated and an "effective conical angle" is defined. This "effective conical angle" is the angle formed by a solid conical structure having a transmission line impedance equal to that of the sparse structure. With the sparse structure defined in terms of an equivalent solid structure, one can better design and calculate the response of the more realistic structures used to approximate conical antennas.

This note deals specifically with N small wires spaced at equal angles around the surface of a cone. The axis of the cone is perpendicular to a ground plane which intersects the apex of the cone (see Figure 1). In order to make the fields independent of the distance along the axis of the cone, each of the small wires is first approximated by a thin cone and the effect due to the wires actually being cylindrical is considered later. The effective conical angle of such a sparse cone is calculated and the data presented in the attached graphs with the number and size of the wires as parameters.

II. Method of Solution

The method used for considering a TEM wave on a solid conical antenna above a ground plane involves treating the cone and ground plane as the plates of a conical transmission line.^{1,2,3} If the spherical coordinates (r, θ, ϕ) are used in the conical system, an equivalent cylindrical transmission line with coordinates (ρ, ϕ, z') is generated by the transformations

$$\rho = 2z_0 \tan \frac{\theta}{2} \quad (1)$$

$$\phi = \phi \quad (2)$$

and

$$z' = r$$

(3)

where z_0 is an arbitrary constant. This transformation maps a cone above a ground plane into a coaxial line since both the cone and ground plane are surfaces of constant θ .

Now consider the case of N small wires whose centers lie on a cone above a ground plane. If we apply the above transformations, the ground plane will again map into a circular cylinder and the center of each wire will map onto a point on a cylinder coaxial and within the cylinder formed by the ground plane. However, if the wires are cylindrical, their surfaces are transformed into surfaces whose cross-sections are functions of z' . One prefers the cross-sections to be independent of z' so that we only have a two-dimensional problem and the techniques of complex variable conformal mapping can be used. Since it is assumed that the N wires are all thin, one can approximate each wire by a very narrow cone of half-angle θ_1 . [The effects of this approximation will be considered later.] When transformed to the cylindrical system such narrow cones have cross-sections independent of z' , as desired.

Thus, the transformations in equations 1, 2, and 3 give us an equivalent cylindrical transmission line consisting of N equally spaced parallel conductors within a cylindrical conductor (see Figure 2). One must now find a potential distribution such that the conductor surfaces match equipotential lines. To do this one must first consider exactly what cross-sectional shapes the thin cones approximating the wires map into.

Obviously, in the limit that θ_1 goes to zero the cross-section just goes to a point. Thus, for small θ_1 one can expect that the cross-section of each wire could be approximated rather well by a circle. Now consider describing the cross-section more exactly. A cross-section at constant z' is equivalent to the transformation of the cross-section of the thin cone at a constant radius r . At a constant r , the surface of a thin cone can be described in terms of θ and ϕ and the transformations in equations 1, 2, and 3 applied to obtain the cylindrical cross-section. Consider a thin cone of half-angle θ_1 inclined at an angle θ_0 with respect to the z -axis (see Figure 3). A surface of constant r intersects the surface of this cone along a circle. Let α_p be an angle measured in the plane of the circle from its center, where α_p is measured with respect to a plane passing through the center of the circle and the z -axis. The angle α_p indicates the location of some point P on the circle, and with sufficient effort, one can show that θ_p and ϕ_p describing the point P are given by the expressions

$$\theta_P = \tan^{-1} \left[\frac{\sin\theta_o \cos\theta_1 - \sin\theta_1 \cos\theta_o \cos\alpha_P}{\cos\theta_o \cos\theta_1 + \sin\theta_o \sin\theta_1 \cos\alpha_P} \cdot \frac{1}{\cos\phi_P} \right] \quad (4)$$

where

$$\phi_P = \tan^{-1} \left[\frac{\sin\theta_1 \sin\alpha_P}{\sin\theta_o \cos\theta_1 - \sin\theta_1 \cos\theta_o \cos\alpha_P} \right] \quad (5)$$

Thus we have descriptions for (θ_P, ϕ_P) in terms of the parameter α_P which simply varies from 0 to 2π radians. Applying equations 1 and 2 to the above equations gives the cylindrical cross-section achieved by transforming such a cone.

Note that for small θ_1 , equations 4 and 5 can be written as

$$\theta_P \approx \tan^{-1} \left[\frac{\sin\theta_o - \theta_1 \cos\theta_o \cos\alpha_P}{\cos\theta_o + \sin\theta_o \cos\alpha_P} \cdot \frac{1}{\cos\phi_P} \right] \quad (6)$$

$$\phi_P \approx \frac{\theta_1 \sin\alpha_P}{\sin\theta_o - \theta_1 \cos\theta_o \cos\alpha_P} \quad (7)$$

It can be seen by considering the above relations that a thin cone will approximate a circular cylinder when transformed as described. What one now needs is a simple expression for the effective radius of the circular cylinder.

Along the radial direction, one can define a radius R_r given by the expression

$$2R_r = 2z_o \tan\left(\frac{\theta_o + \theta_1}{2}\right) - 2z_o \tan\left(\frac{\theta_o - \theta_1}{2}\right) \quad (8)$$

$$= 2z_o \frac{\sin\theta_1}{\cos\left(\frac{\theta_o + \theta_1}{2}\right) \cos\left(\frac{\theta_o - \theta_1}{2}\right)} \quad (9)$$

which, for small θ_1 becomes

$$R_r \approx z_o \frac{\theta_1}{\cos^2 \frac{\theta_o}{2}} = \frac{2z_o \theta_1}{1 + \cos \theta_o} \quad (10)$$

Similarly, along the azimuthal direction (ϕ -direction) one has a radius R_ϕ , where

$$R_\phi \approx \left[2z_o \tan \frac{\theta_o}{2} \right] \phi_1 \quad (11)$$

where ϕ_1 is the half-angle subtended by the thin cone when viewed from the z -axis. It is easily seen that for small θ_1

$$\phi_1 \approx \frac{\theta_1}{\sin \theta_o} \quad (12)$$

so that

$$R_\phi \approx 2z_o \tan \left(\frac{\theta_o}{2} \right) \frac{\theta_1}{\sin \theta_o} \quad (13)$$

$$= \frac{2z_o \theta_1}{1 + \cos \theta_o} \quad (14)$$

From equations 10 and 14, one discovers that

$$R_\phi = R_r \quad (15)$$

Therefore, in the two orthogonal directions considered, the radii of the cross-sections of the transformed thin cones are equal, at least in the limit of small θ_1 . Thus, one can define an effective circular radius as

$$R_{\text{eff}} = \frac{2z_o \theta_1}{1 + \cos \theta_o} \quad (16)$$

Now the problem becomes one of finding the potential distribution due to N parallel wires of radius R_{eff} equally spaced along the circumference of a circle of radius R_1 , all within a coaxial conducting cylinder of radius R_2 (see Figure 2). For

convenience, let $R_2 = 1$, which is equivalent to picking z_0 in equation 1 equal to $1/2$, or just dividing all radii by R_2 .

Consider the conformal transformation*

$$w = \frac{1}{N} \ln \left[\left(\frac{\zeta}{R_1} \right)^N - 1 \right] - \frac{1}{N} \ln \left[(\zeta R_1)^N - 1 \right] \quad (17)$$

where

$$w = u + iv \quad (18)$$

$$\zeta = x + iy = \rho e^{i\phi} \quad (19)$$

Now w is singular at the points

$$\frac{\zeta}{R_1} = 1^{1/N} = e^{\frac{2\pi n}{N} i} \quad (20)$$

$$\zeta R_1 = 1^{1/N} = e^{\frac{2\pi n}{N} i} \quad (21)$$

for $n = 0, 1, 2, \dots, N - 1$.

The points defined by equation 20 correspond to the centers of the N wires. The singular points in equation 21 refer to images of the wires outside the unit cylinder. These image locations are necessary to ensure that the surrounding unit cylinder is an equipotential and correspond to images of the N wires below the ground plane in the initial conical geometry.

Now, separating the real and imaginary parts of w one gets

$$u = \frac{1}{2N} \ln \left[\frac{\left(\frac{\rho}{R_1} \right)^{2N} - 2\cos(N\phi) \left(\frac{\rho}{R_1} \right)^N + 1}{(\rho R_1)^{2N} - 2\cos(N\phi) (\rho R_1)^N + 1} \right] \quad (22)$$

*Compare to equation 43 of Reference 4.

$$v = \frac{1}{N} \left\{ \tan^{-1} \left[\frac{\left(\frac{\rho}{R_1}\right)^N \sin N\phi}{\left(\frac{\rho}{R_1}\right)^N \cos N\phi - 1} \right] - \tan^{-1} \left[\frac{(\rho R_1)^N \sin N\phi}{(\rho R_1)^N \cos N\phi - 1} \right] + \pi k \right\} \quad (23)$$

$$k = 0, 1, 2, \dots, N - 1$$

Note that at $\rho = 1$, u goes to a constant value for all ϕ ; i.e.,

$$u_1 \equiv u(\rho = 1, \phi) = \frac{1}{2N} \ln \left[\frac{1}{R_1^{2N}} \right] = \ln \left(\frac{1}{R_1} \right) \quad (24)$$

This ensures that the surface $\rho = 1$ is an equipotential. We now require the potential on the surfaces of each wire; i.e., the potential a distance R_{eff} from each of the singular points at

$$R_1 e^{\frac{2\pi n}{N} i}.$$

Define a new complex variable v by

$$\zeta \equiv R_1 (1 + v) \quad (25)$$

Then

$$w = \frac{1}{N} \ln \left[\frac{(1+v)^N - 1}{R_1^{2N} (1+v)^N - 1} \right] \quad (26)$$

where for small v ,

$$w = \frac{1}{N} \ln \left[\frac{Nv + O(v^2)}{R_1^{2N} (1 + Nv) - 1 + O(v^2)} \right]$$

$$= \frac{1}{N} \ln [Nv] - \frac{1}{N} \ln \left[R_1^{2N} - 1 + R_1^{2N} Nv \right] + O(v) \quad (27)$$

Thus in the limit as $v \rightarrow 0$, u has the asymptotic form

$$u \approx \frac{1}{N} \ln[N|v|] - \frac{1}{N} \ln \left[|R_1^{2N} - 1 + R_1^{2N} N v| \right] \quad (28)$$

Setting $u = u_0$ and $|v| = R_{eff}/R_1$ we have the potential u_0 on the surface of each of N wires.

$$u_0 \approx \frac{1}{N} \ln \left(\frac{NR_{eff}}{R_1} \right) - \frac{1}{N} \ln \left[1 - R_1^{2N} \right] \quad (29)$$

where we have assumed $NR_{eff}/R_1 \ll 1$, which corresponds to the assumption that θ_1 is small ($\theta_1 \ll 1$).

The transmission line being considered is characterized by a geometrical factor f_g where⁵

$$f_g = \frac{\Delta u}{\Delta v} \quad (30)$$

where

Δu is the difference in the potential function, u , between one of the center conductors and the outer conductor, and

Δv is the change in the stream function, v , on a path circling the N interior conductors.

Thus defined,

$$f_g = \frac{u_1 - u_0}{2\pi} \quad (31)$$

$$= \frac{1}{2\pi} \ln \left[\frac{1}{R_1} \right] - \frac{1}{2\pi} \ln \left[(1 - R_1^{2N})^{1/N} \right] \quad (32)$$

$$- \frac{1}{2\pi} \ln \left[\left(\frac{NR_{eff}}{R_1} \right)^{1/N} \right]$$

$$= \frac{1}{2\pi} \ln \left\{ \frac{\frac{1}{R_1}}{\left[\frac{NR_{eff}}{R_1} (1 - R_1^{2N}) \right]^{1/N}} \right\} \quad (33)$$

Now, remember that

$$R_1 = 2z_0 \tan \frac{\theta_0}{2} \quad (34)$$

and for the choice of $z_0 = 1/2$ so that R_2 would equal 1, we get the expression

$$f_g = \frac{1}{2\pi} \ln \left\{ \frac{\cot \frac{\theta_0}{2}}{\left[\frac{NR_{\text{eff}}}{\tan \frac{\theta_0}{2}} \left(1 - \tan^{2N} \left(\frac{\theta_0}{2} \right) \right) \right]^{1/N}} \right\} \quad (35)$$

where

$$R_{\text{eff}} = \frac{\theta_1}{1 + \cos \theta_0} \quad (36)$$

Note that for large N

$$\left[1 - \tan^{2N} \left(\frac{\theta_0}{2} \right) \right]^{1/N} \rightarrow 1 \quad (37)$$

and

$$f_g \approx \frac{1}{2\pi} \ln \left\{ \frac{\cot \frac{\theta_0}{2}}{\left[\frac{NR_{\text{eff}}}{\tan \left(\frac{\theta_0}{2} \right)} \right]^{1/N}} \right\} \quad (38)$$

Now, compare equations 33, 35, and 38 to equation 58 of reference 4. Reference 4 gives the equivalent radius of a cylinder made of N parallel wires as

$$\psi_{\text{eq}} = \psi_1 \left(\frac{Nr_1}{\psi_1} \right)^{1/N} \quad (39)$$

where ψ_1 is the actual radius of the N-wire cage and r_1 is the individual wire's radius. Note that we have a very similar expression in equation 33 if we replace R_1 by ψ_1 and R_{eff} by r_1 . The only difference is the factor

$$(1 - R_1^{2N})^{1/N}$$

which comes from the image of the wires below the ground plane. And from equation 37, this difference has little effect if one has a large number of wires, N.

Now consider a solid cone above a ground plane and the equivalent angle, θ_{eq} , that would give the same geometrical factor as above. The geometrical factor for a solid cone is just 1,2,6

$$f_g \text{ (solid cone)} = \frac{1}{2\pi} \ln \left[\cot \frac{\theta_{eq}}{2} \right] \quad (40)$$

Therefore, θ_{eq} can be written in terms of θ_0 by equating the geometrical factors for a N-wire cone and a solid cone. Thus

$$\cot \frac{\theta_{eq}}{2} = \frac{\cot \frac{\theta_0}{2}}{\left[\frac{NR_{eff}}{\tan\left(\frac{\theta_0}{2}\right)} \left(1 - \tan^{2N}\left(\frac{\theta_0}{2}\right)\right) \right]^{1/N}} \quad (41)$$

which gives

$$\theta_{eq} = 2 \tan^{-1} \left\{ \frac{\left[NR_{eff} \left(1 - \tan^{2N}\left(\frac{\theta_0}{2}\right)\right) \right]^{1/N}}{\left[\tan\left(\frac{\theta_0}{2}\right) \right]^{\frac{1-N}{N}}} \right\} \quad (42)$$

Thus one can characterize an N-wire cone by an equivalent solid cone with the half-angle θ_{eq} given by equation 41. Figures 4-13 give θ_{eq} for various θ_0 with N and θ_1 as parameters. Note that the above equations are not valid for very small θ_0 (where the narrow cones almost touch) or for θ_0 near $\pi/2$ (where the

thin cones almost touch the ground plane). For this reason the attached graphs are not plotted for θ_0 very near to 0 or $\pi/2$.

III. Results

The calculation of θ_{eq} in equation 41 indicates that a sparse cone of N-wires and half-angle θ_0 is equivalent to a thinner solid cone of half-angle θ_{eq} ; i.e., $\theta_{eq} < \theta_0$. One might also think in terms of pulse impedance, Z , where

$$Z = \sqrt{\frac{\mu_0}{\epsilon_0}} f_g \approx 120\pi f_g \quad (43)$$

By comparing the geometrical factors of sparse and solid cones it can be seen that a sparse cone must have a larger half-angle than a solid cone in order for the two to have the same impedance (see Figure 14).

Now consider the effects of using cylindrical wires of radius r_0 in actually building a sparse cone rather than thin cones of half-angle θ_1 . The effect is obviously greatest at the apex of the cone since wires with a finite radius cannot meet at a point as the thin cones were assumed to do. A long distance along the cone, however, the thin wires can be modeled fairly well by narrow cones. In fact, it can readily be seen that the geometrical factor (and thus the pulse impedance) is actually a function of the distance z along the axis of the cone when cylindrical wires are used. At a given z the angle θ_1 subtended by a wire of radius r_0 passing through the origin at an angle θ_0 with respect to the z -axis is approximately given by

$$\theta_1 \approx \frac{r_0 \cos \theta_0}{z} \quad (44)$$

where we require θ_1 to be small. This implies that

$$\frac{r_0}{z} \ll 1 \quad (45)$$

and thus does not apply for z near zero. In the limit that equation 44 is correct, one can get an approximation for the geometrical factor and the impedance by simply placing the expression for θ_1 of equation 43 into equation 36, giving

$$R_{\text{eff}} = \frac{r_o \cos \theta_o}{z[1 + \cos \theta_o]} \quad (46)$$

Then Z , θ_{eq} , and f_g all become functions of both θ_o and z rather than of θ_o alone. It is readily seen that for $z \gg r_o$, the impedance changes relatively slowly with z . In real cases we are probably dealing with a truncated conical antenna and it is a pretty good approximation just to replace z in equation 44 by the height, h , of the antenna; i.e., use

$$\theta_1 \approx \frac{r_o \cos \theta_o}{h} \quad (47)$$

This approximation is good when $r_o/h \ll 1$.

Now let us consider what curve each wire of an N -wire cone should follow to obtain a constant impedance structure. To do this, place the expression for R_{eff} of equation 46 into equation 35. Using equation 42, one obtains

$$Z = 60 \ln \left\{ \frac{\cot\left(\frac{\theta_o}{2}\right)}{\left[\frac{Nr_o \cos \theta_o \left[1 - \tan^{2N}\left(\frac{\theta_o}{2}\right)\right]}{z \tan\left(\frac{\theta_o}{2}\right) [1 + \cos \theta_o]} \right]^{1/N}} \right\} \quad (48)$$

Assuming a constant impedance, Z , one can solve for z in terms of θ_o .

$$z = Nr_o e^{NZ/60} \left[\frac{\left[1 - \tan^{2N}\left(\frac{\theta_o}{2}\right)\right] \left[\tan^N\left(\frac{\theta_o}{2}\right)\right]}{\tan \theta_o} \right] \quad (49)$$

This gives us the equation for the constant impedance curve in terms of z , the distance along the axis of the N -wire cone, and θ_o , the angle to a point on the curve as measured from the origin (see Figure 15). It is convenient to describe this curve in the Cartesian coordinates (ξ, z) where ξ is the distance perpendicular to the z -axis in the plane of one of the wires making up the cone. Then, it is easily seen that

$$\xi = z \tan \theta_0 = N r_0 e^{NZ/60} \left[\left[1 - \tan^{2N} \left(\frac{\theta_0}{2} \right) \right] \left[\tan^N \left(\frac{\theta_0}{2} \right) \right] \right] \quad (50)$$

Note that the expressions for z and ξ are only valid if

$$z \gg r_0, \quad \xi \gg r_0 \quad (51)$$

Thus, the attached plots of constant impedance curves (see Figures 16-17) start out at $\xi = 500 r_0$ to ensure that the above inequalities hold. In any real conical antenna, the area near the apex of the cone would probably be constructed of a solid sheet of metal which would transition to a sparse cone made up of a number of wires at some distance from the apex. Thus, the fact that the above expressions are not valid very near the apex is not particularly critical.

It should be noted that the constant impedance curves plotted are only approximate and the approximations become increasingly worse as the number of wires decreases. This occurs because as the number of wires decreases, the curvature of the constant impedance paths increases. The expression for impedance in equation 43 is based on calculations of the inductance and capacitance per unit length of the transmission line, where for a conical line, the length is measured along the radial direction from the apex. Since the constant impedance paths plotted in Figures 17 and 18 are curved, the distance along the curve is longer than the radial distance to a point on the curve. An exact calculation would have to consider the effects of this difference in path length on transit time, non-TEM mode propagation, etc. However, as long as the number of wires used is not too few, the effect of the curvature on path length is small and the attached plots should be fairly accurate.

IV. Summary

In building EMP simulators and various antenna structures it is often desirable to replace solid conducting surfaces by sparse surfaces to avoid mechanical problems associated with wind loading, weight limitations, etc. In this note we have calculated the effective half-angle of a sparse cone above a ground plane where the sparse cone consists of N thin wires spaced at equal angles around a conical surface. It was seen that a sparse cone is equivalent to a solid cone of smaller half-angle and as one increases N , the number of wires, the sparse cone approaches the limit of a solid cone.

Several limitations exist in these calculations. First of all, it is assumed that the diameter of the wires is small

compared to their separation. Therefore, the approximations used here are not valid for wire separations of the same order as the wire size. Secondly, no consideration has been given to conducting hoops placed at right angles to the wires along the cone. Such hoops might well be added to an actual antenna to better approximate a solid cone, and it is hoped that these effects may be considered in later notes.

References

1. W. R. Smythe, *Static and Dynamic Electricity*, 2nd ed., 1950, p. 479.
2. C. E. Baum, *Sensor and Simulation Note 31, The Conical Transmission Line as a Wave Launcher and Terminator for a Cylindrical Transmission Line*, January 1967.
3. C. E. Baum, *Sensor and Simulation Note 36, A Circular Conical Antenna Simulator*, March 1967.
4. C. E. Baum, *Sensor and Simulation Note 69, Design of a Pulse-Radiating Dipole Antenna as Related to High-Frequency and Low-Frequency Limits*, January 1969.
5. C. E. Baum, *Sensor and Simulation Note 27, Impedances and Field Distributions for Symmetrical Two Wire and Four Wire Transmission Line Simulators*, October 1966.
6. C. E. Baum, *Sensor and Simulation Note 21, Impedances and Field Distributions for Parallel Plate Transmission Line Simulators*, June 1966.

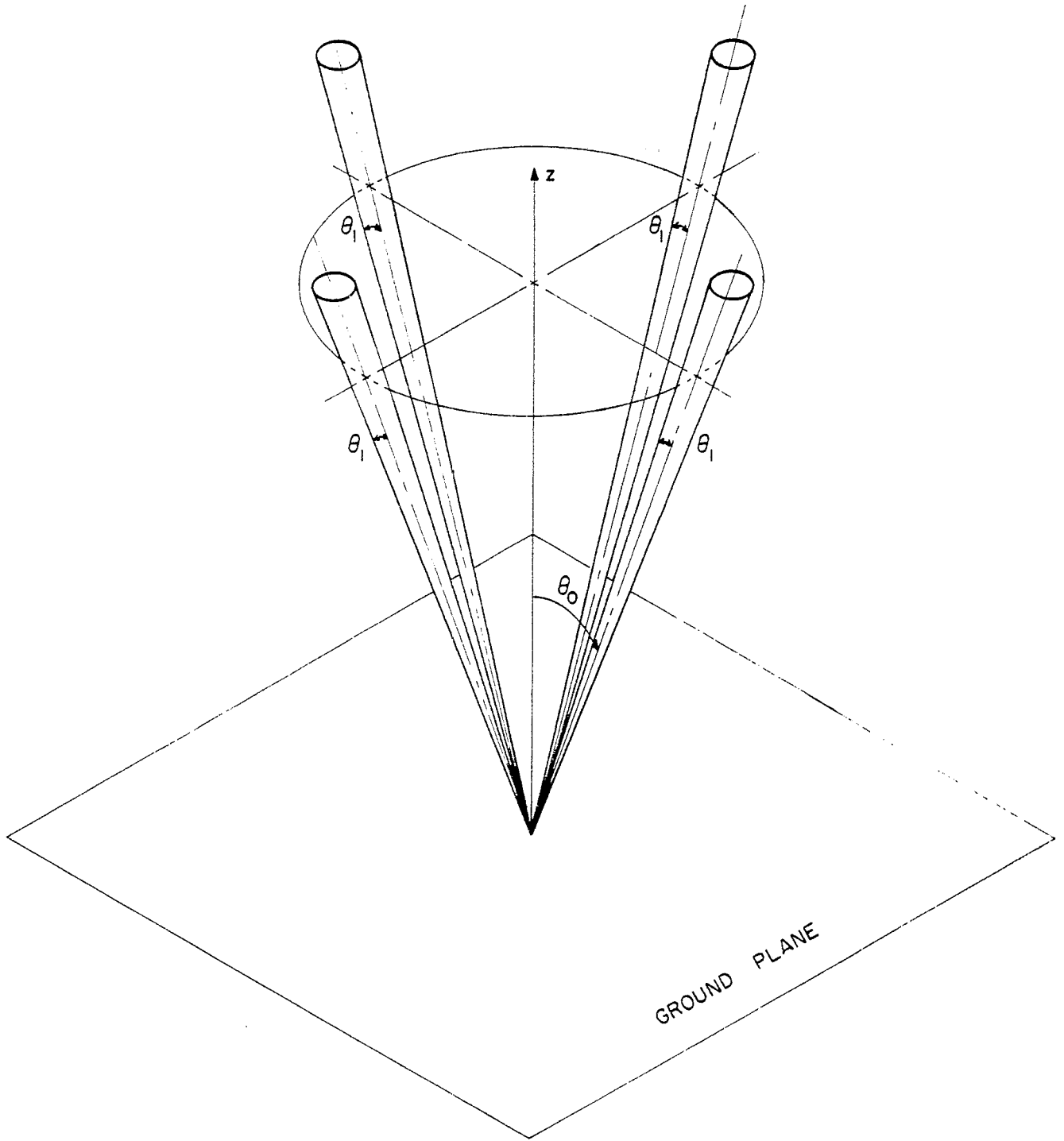


FIGURE 1: 4-WIRE CONE ABOVE A GROUND PLANE

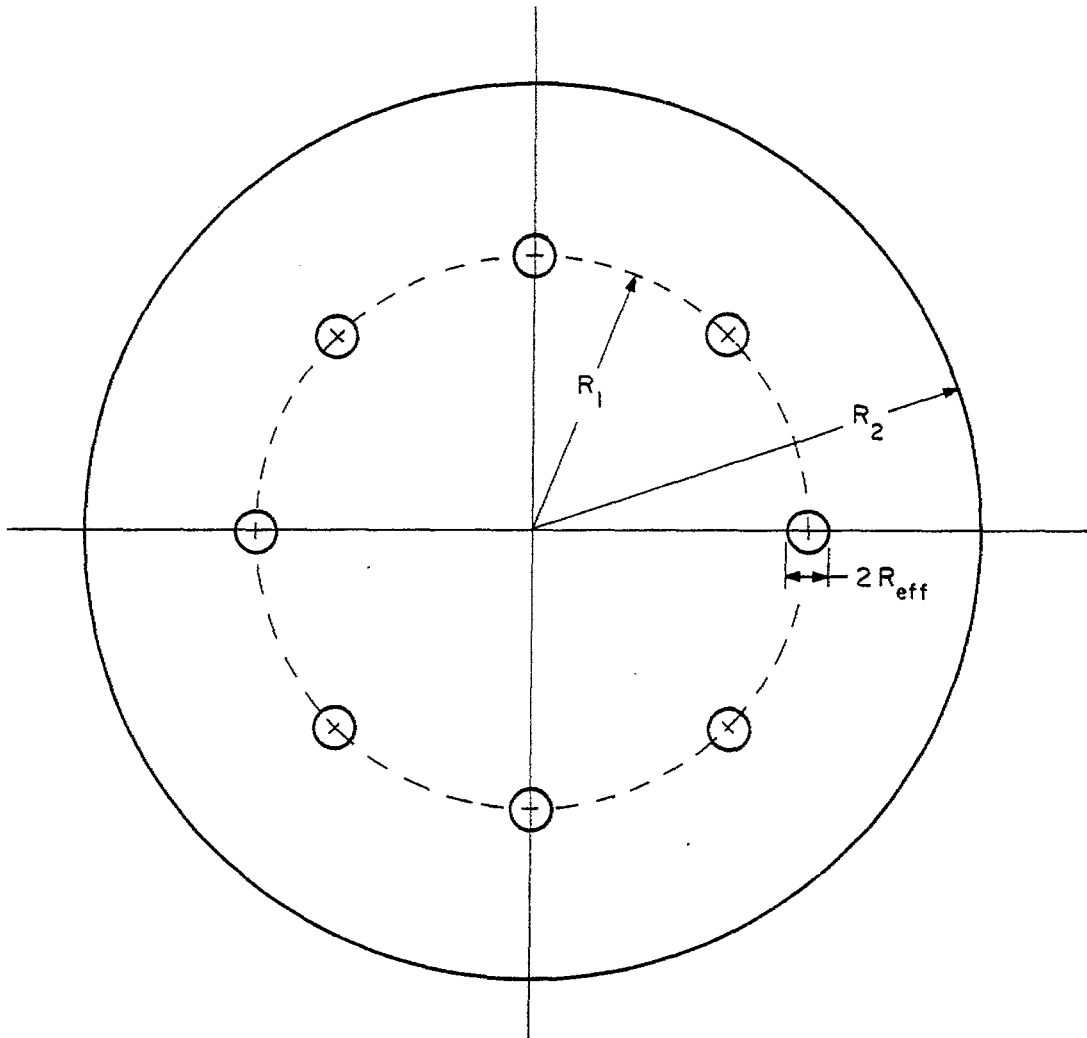


FIGURE 2: EQUIVALENT CYLINDRICAL TRANSMISSION LINE FOR AN 8-WIRE CONE ABOVE A GROUND

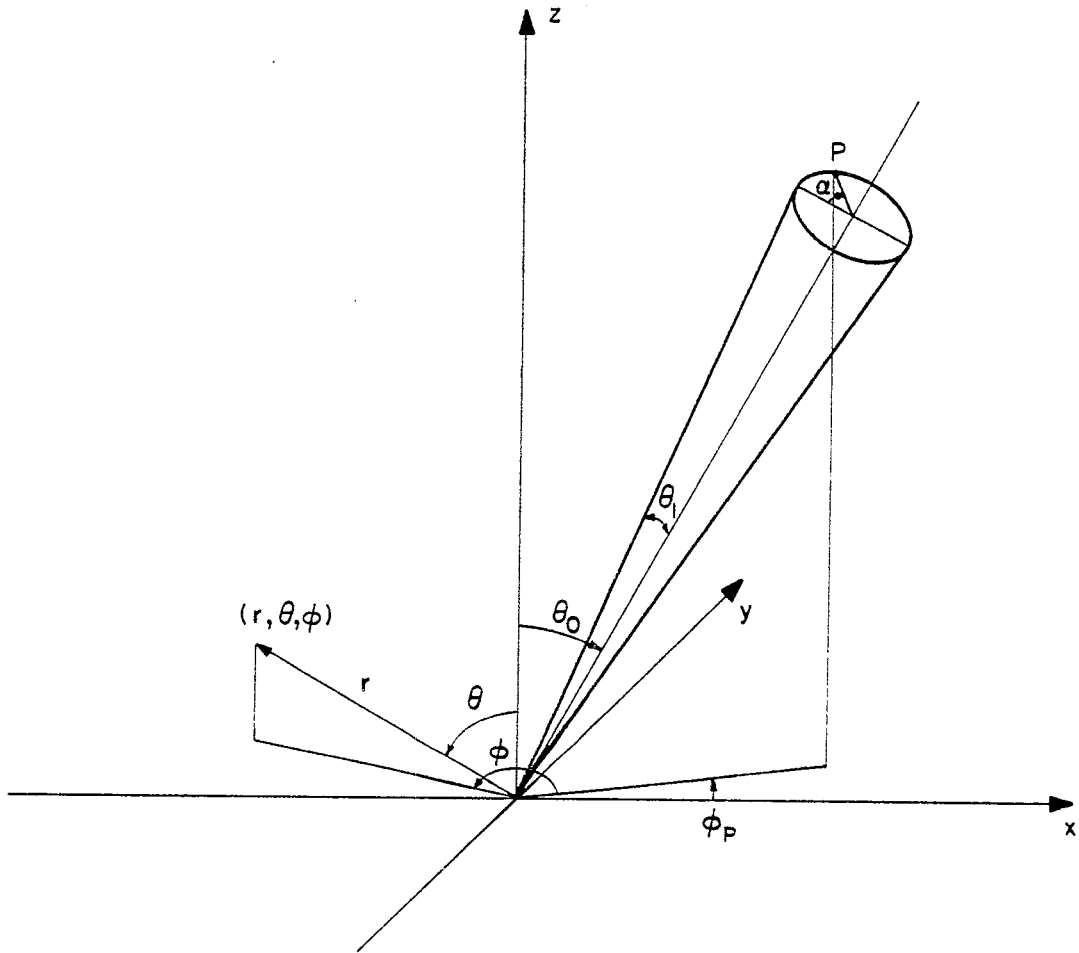


FIGURE 3: CO-ORDINATE SYSTEM DESCRIBING A CONICAL WIRE

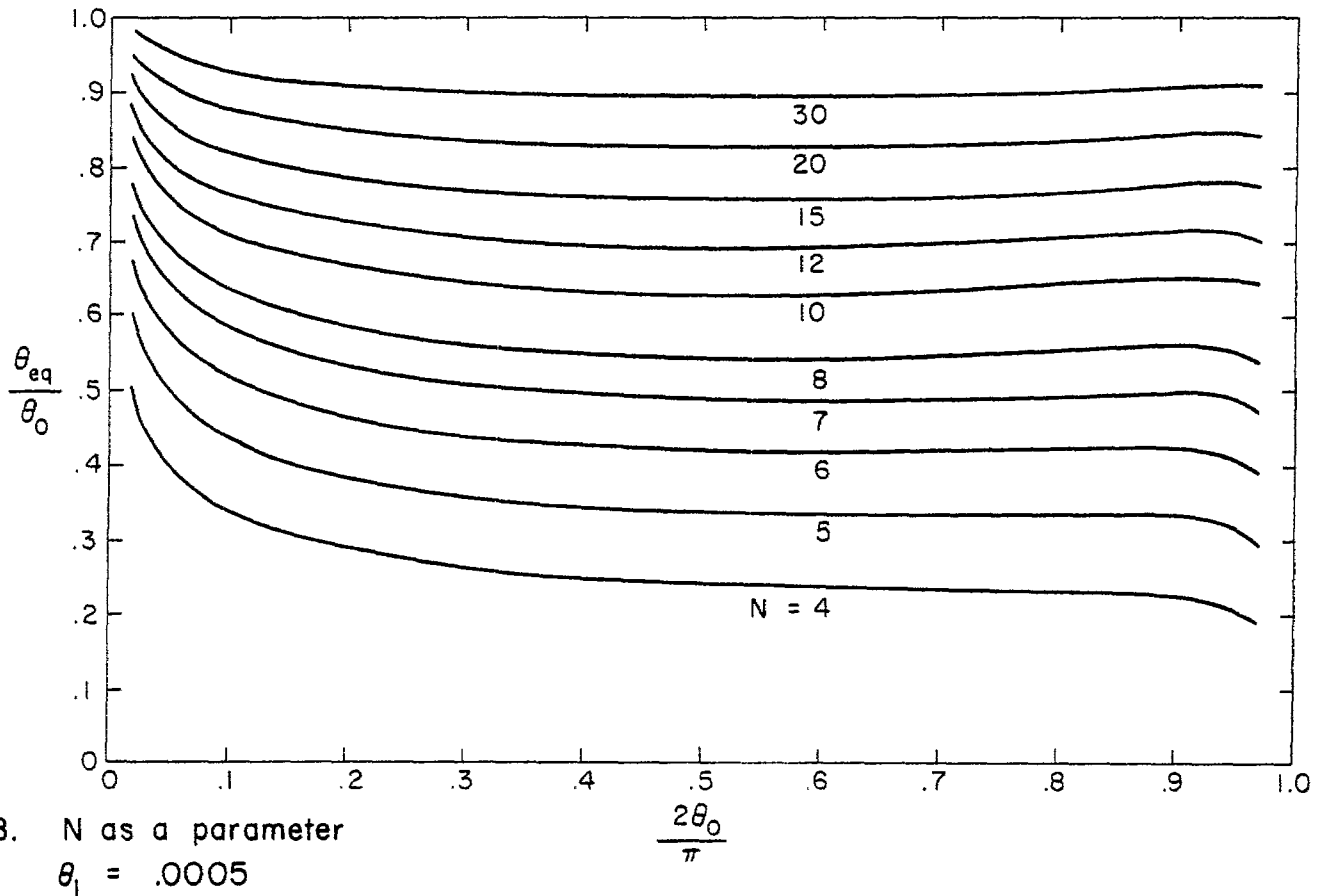
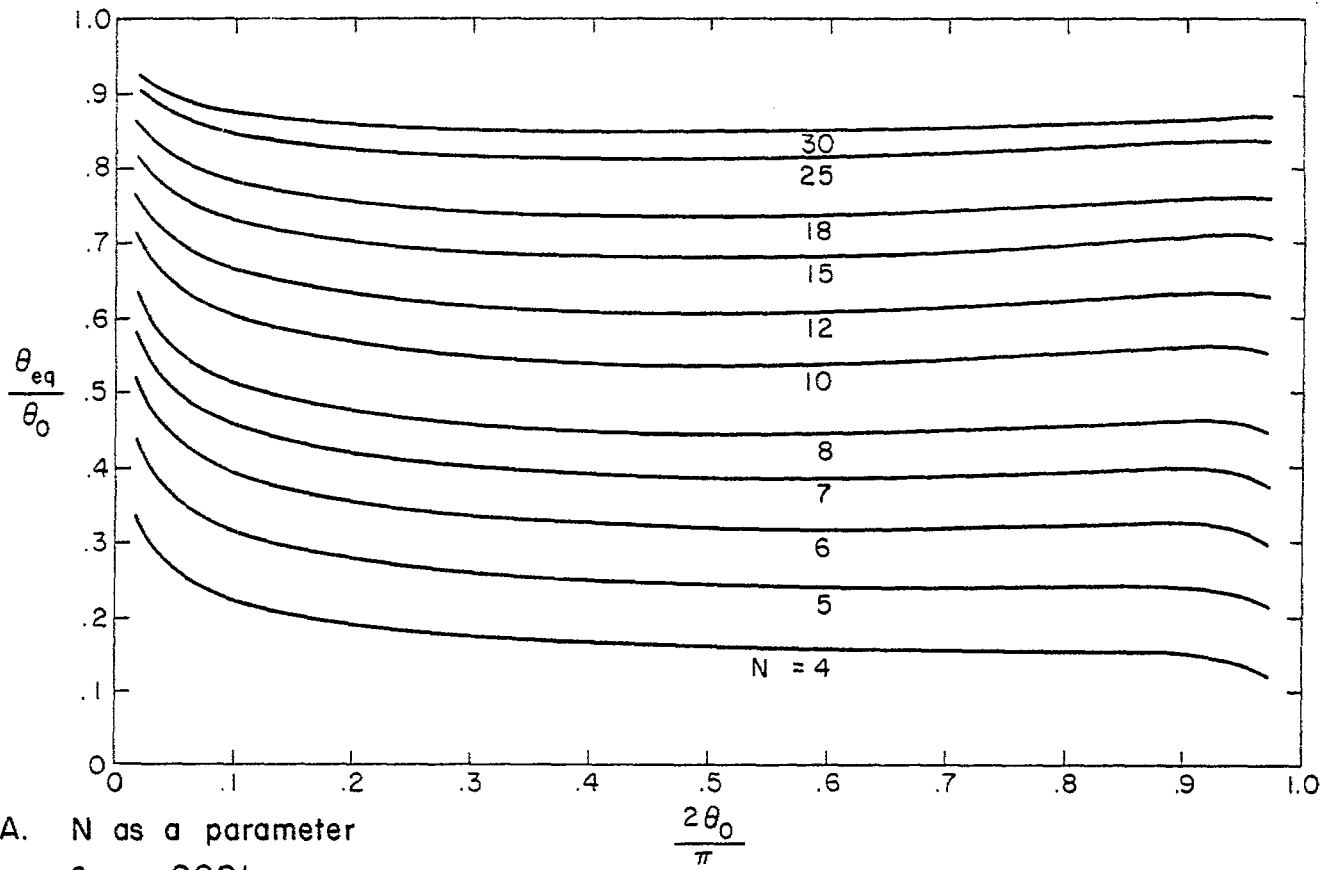


FIGURE 4: EQUIVALENT ANGLE OF A N-WIRE CONE

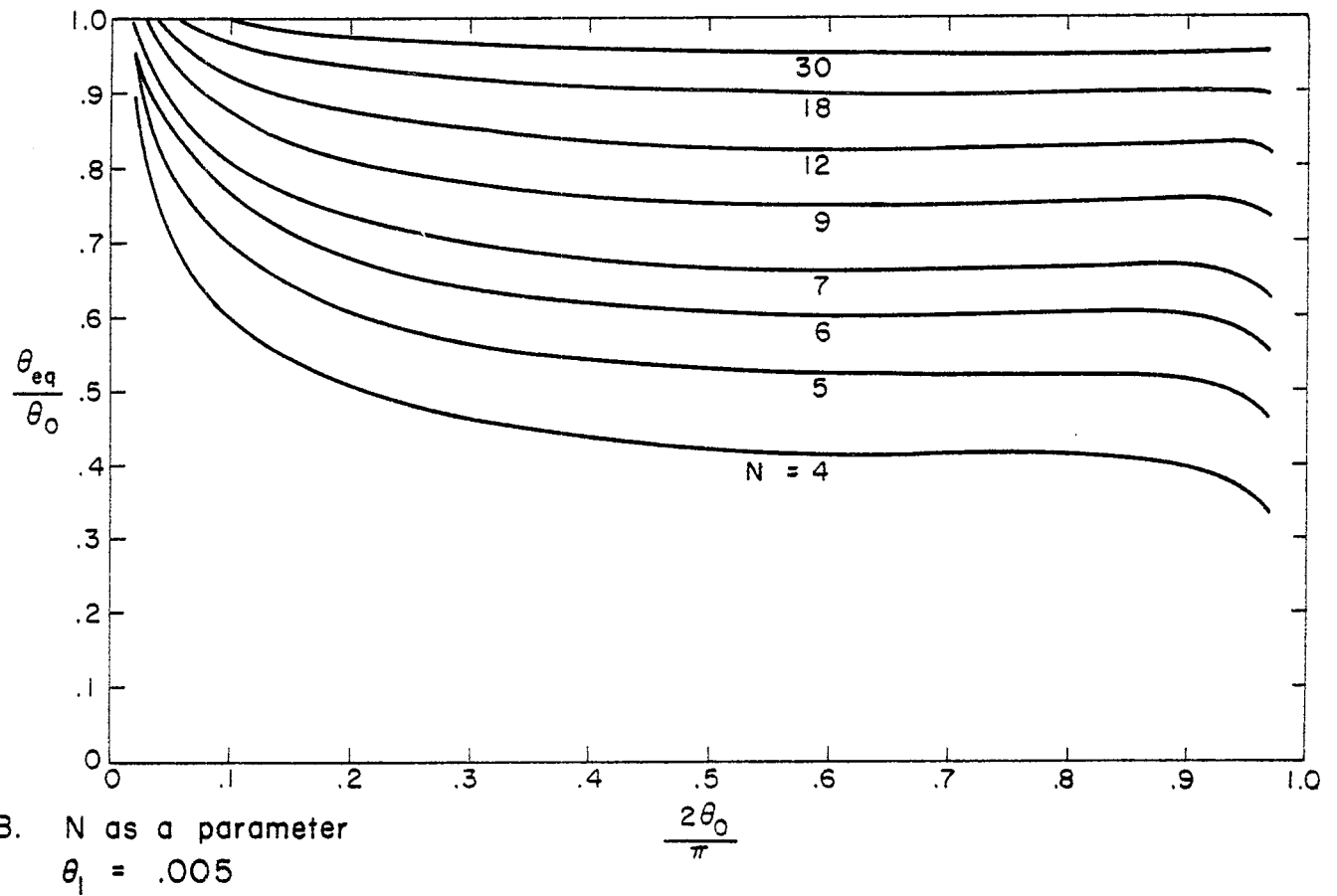
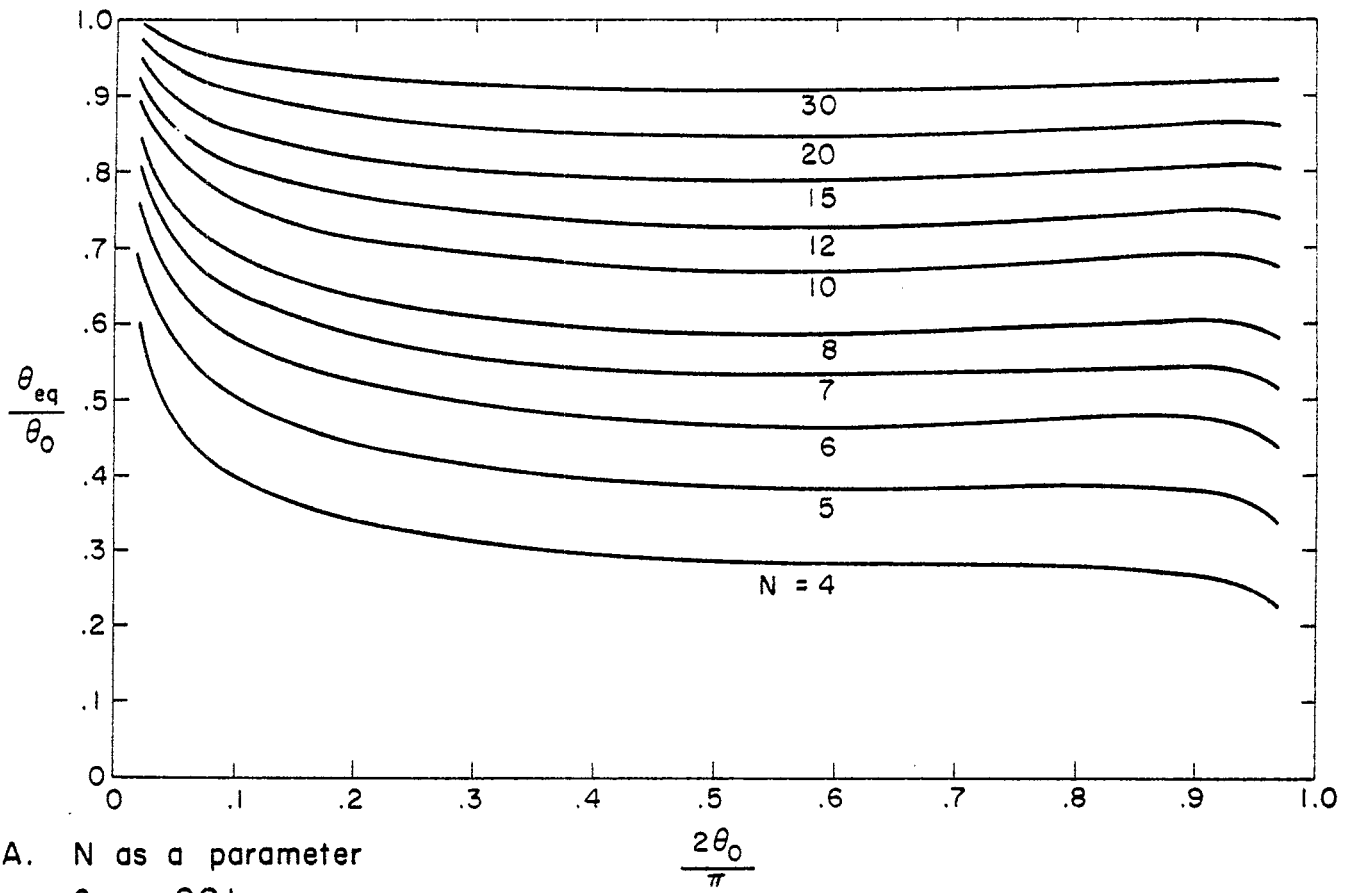


FIGURE 5: EQUIVALENT ANGLE OF A N-WIRE CONE

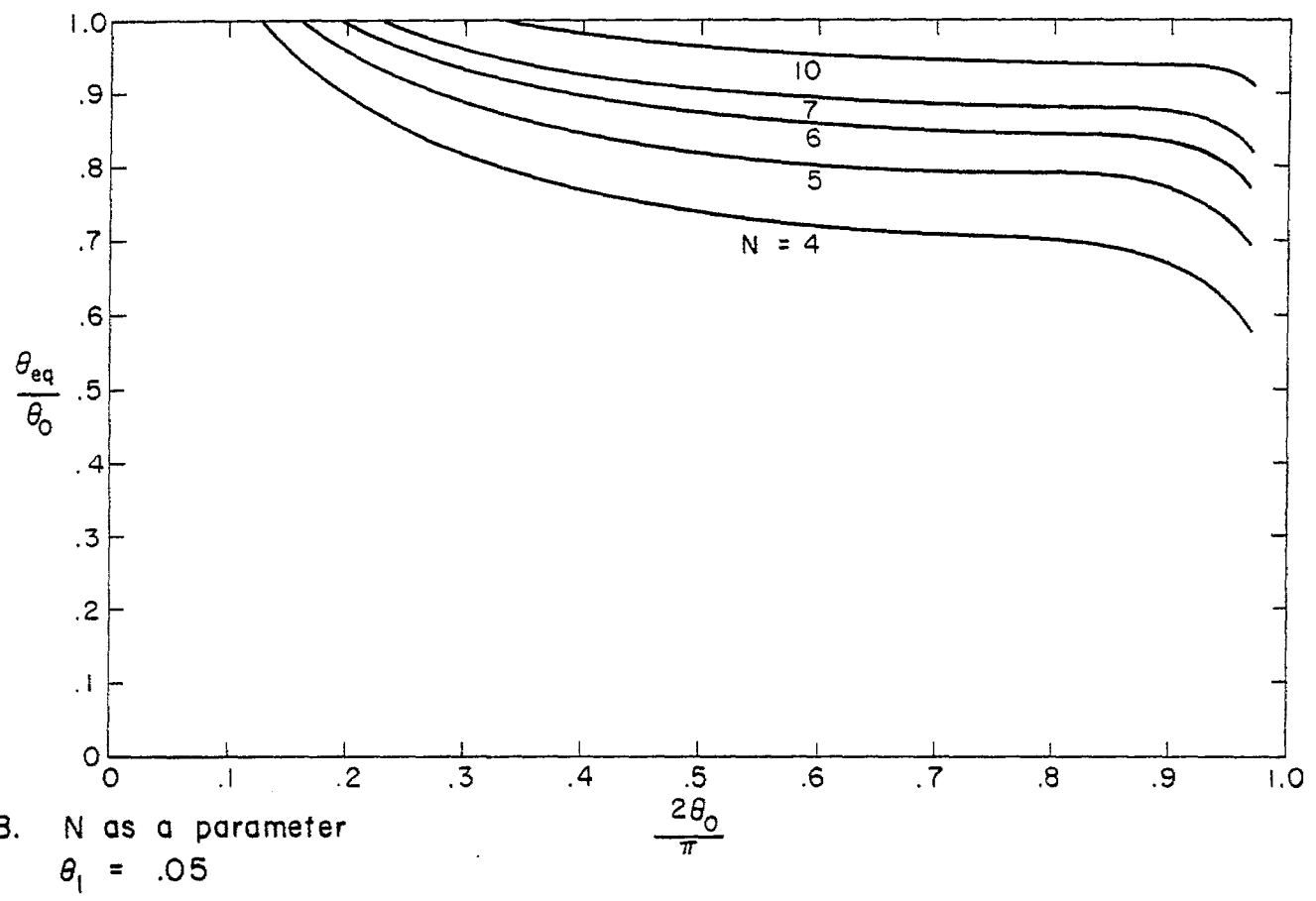
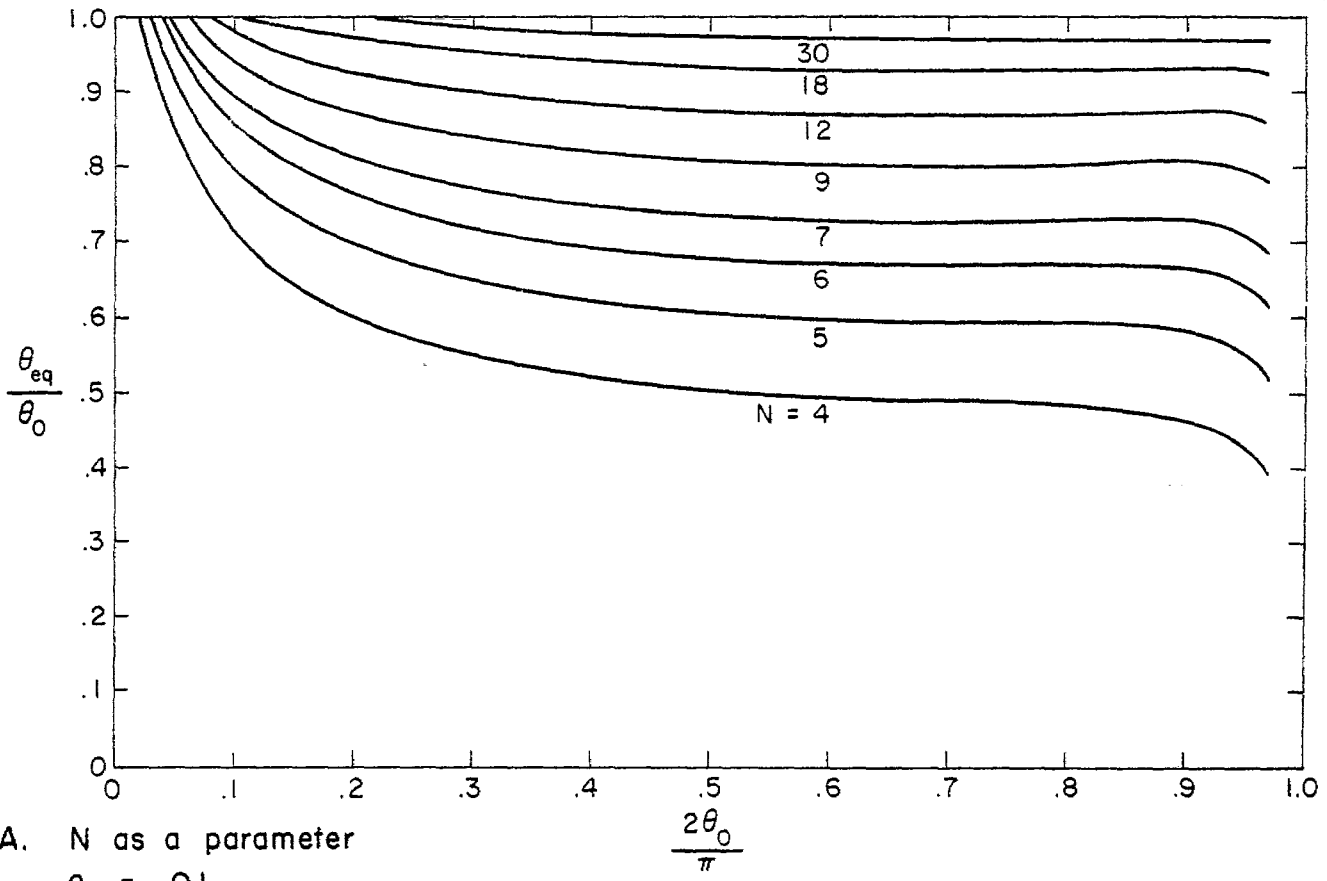


FIGURE 6: EQUIVALENT ANGLE OF A N-WIRE CONE

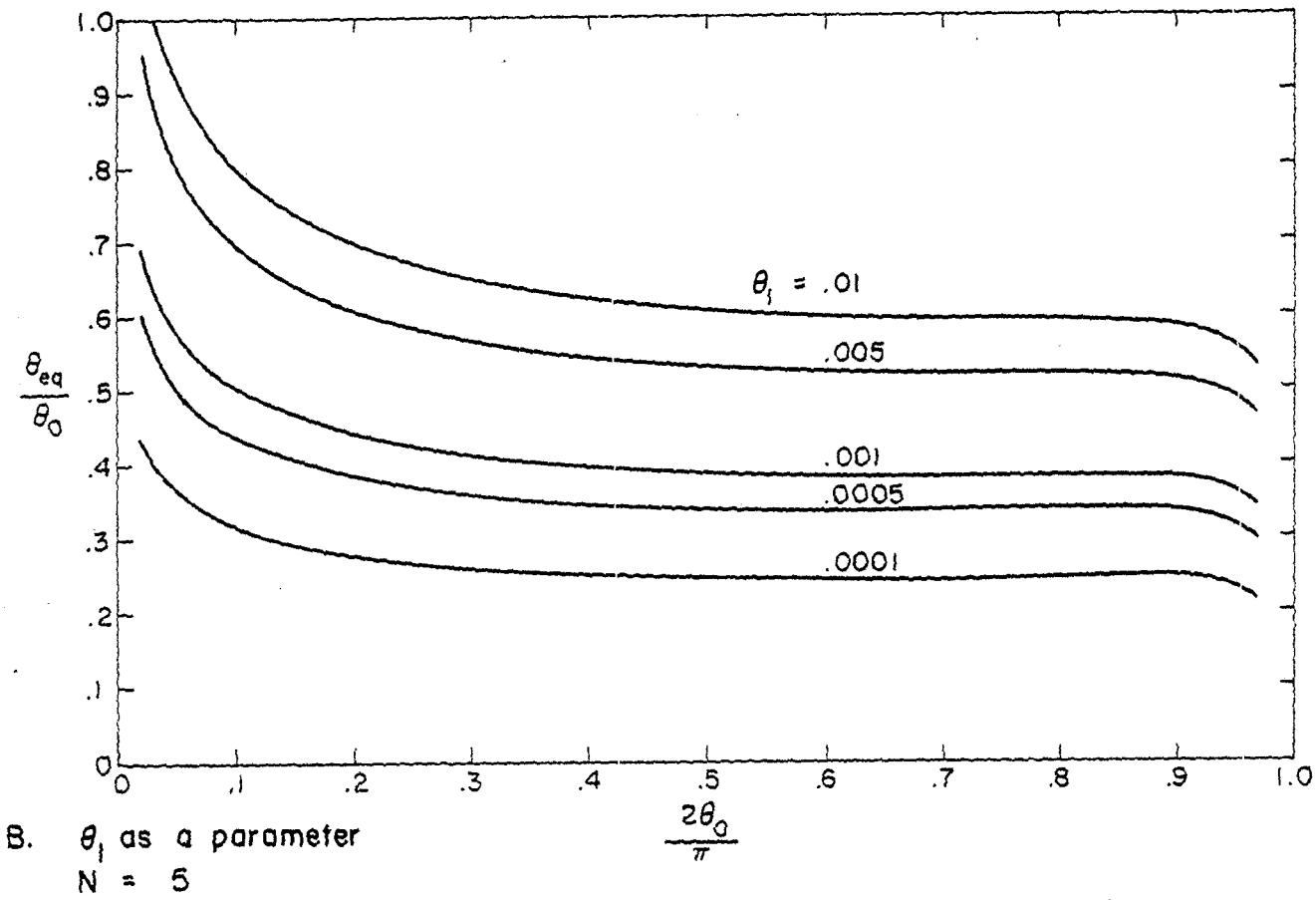
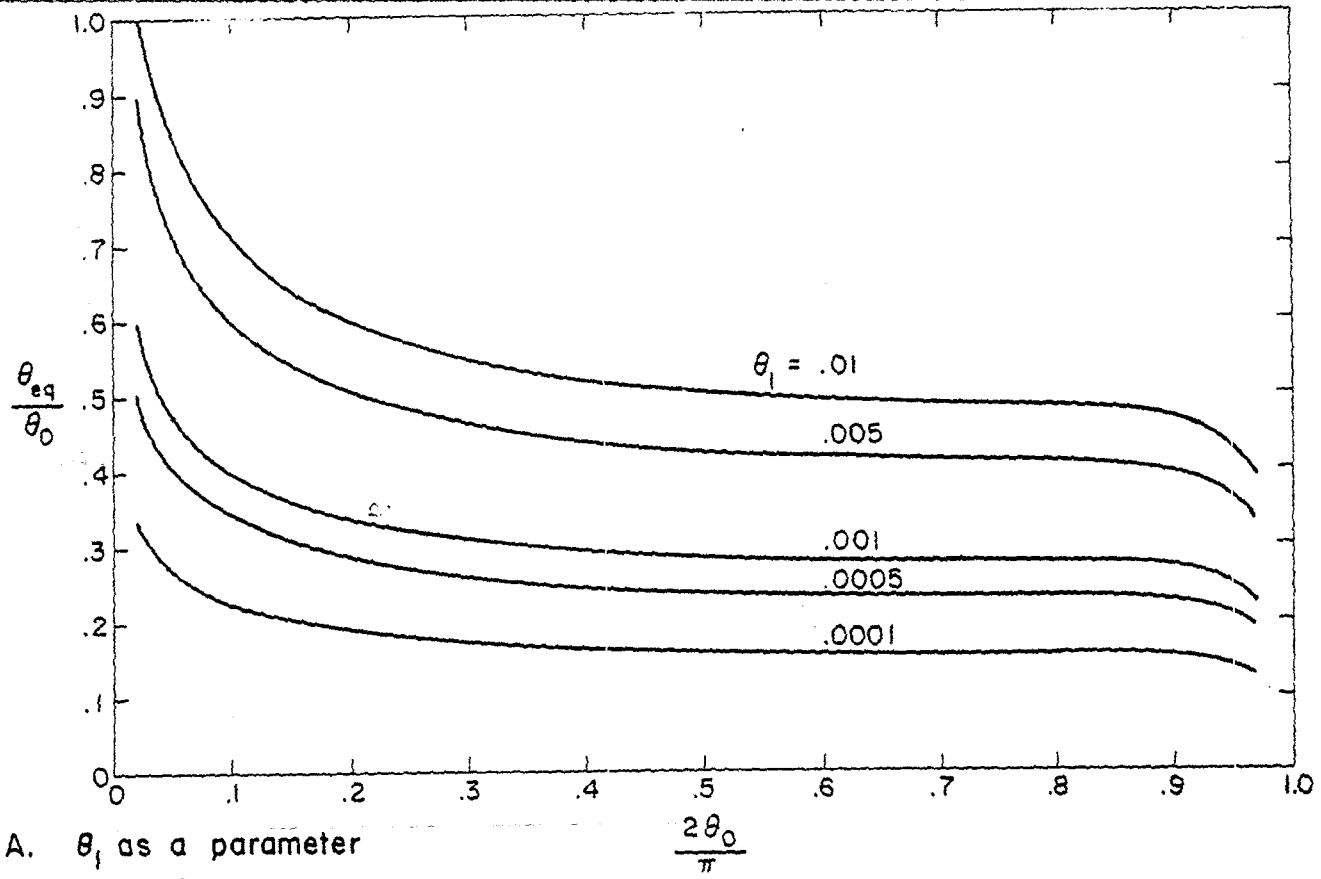
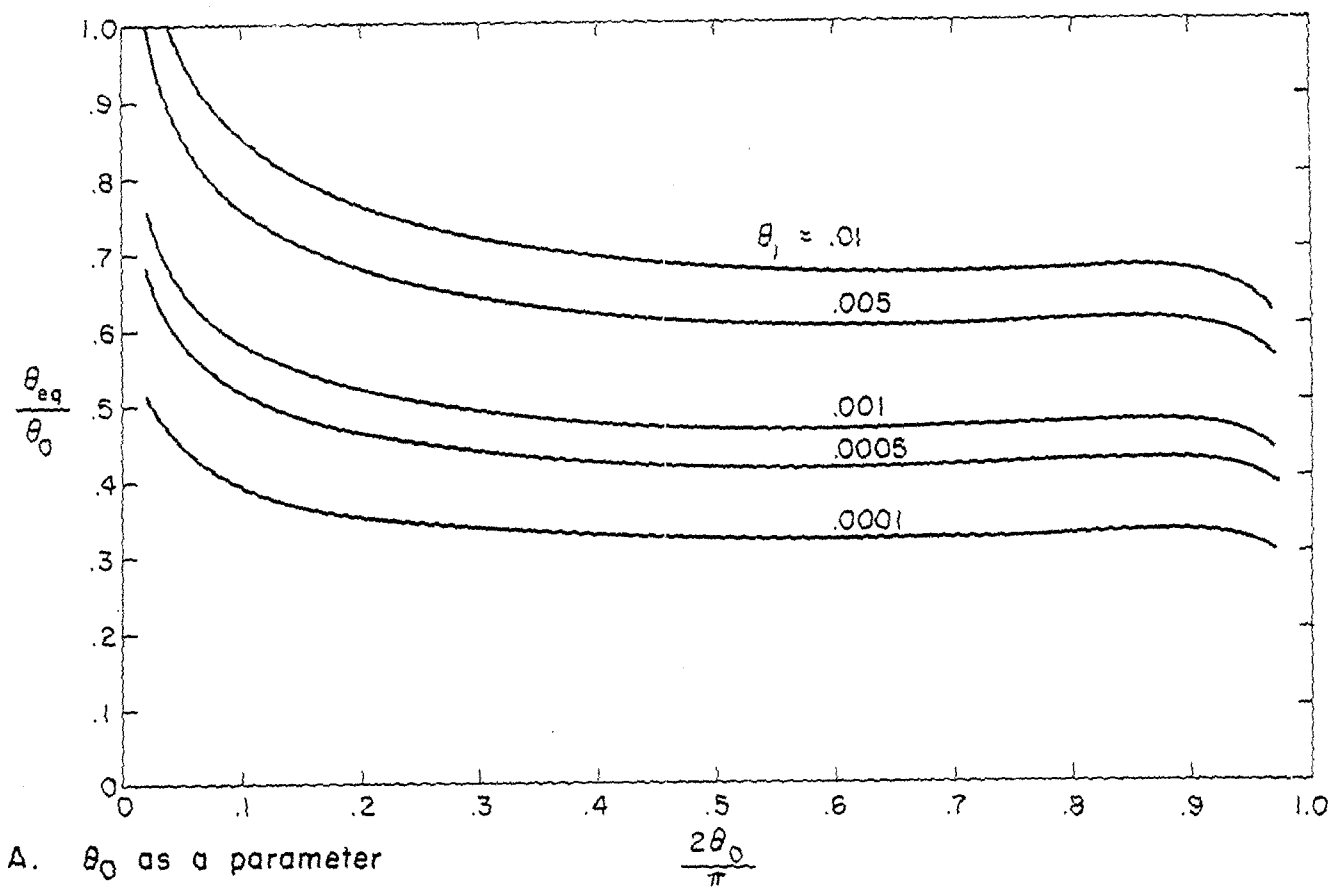
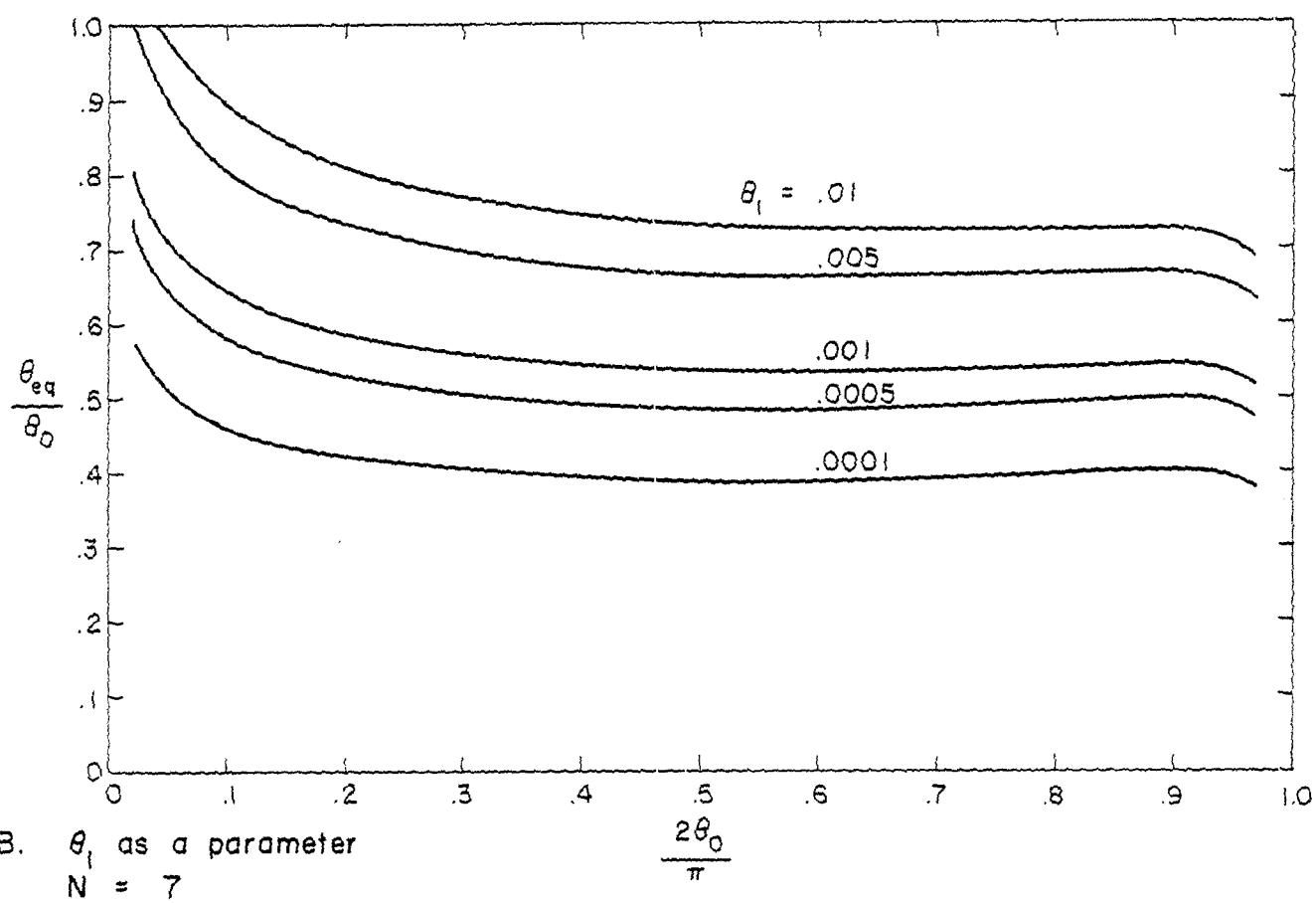


FIGURE 7: EQUIVALENT ANGLE OF A N-WIRE CONE



A. θ_1 as a parameter
 $N = 6$



B. θ_1 as a parameter
 $N = 7$

FIGURE 8: EQUIVALENT ANGLE OF A N-WIRE CONE

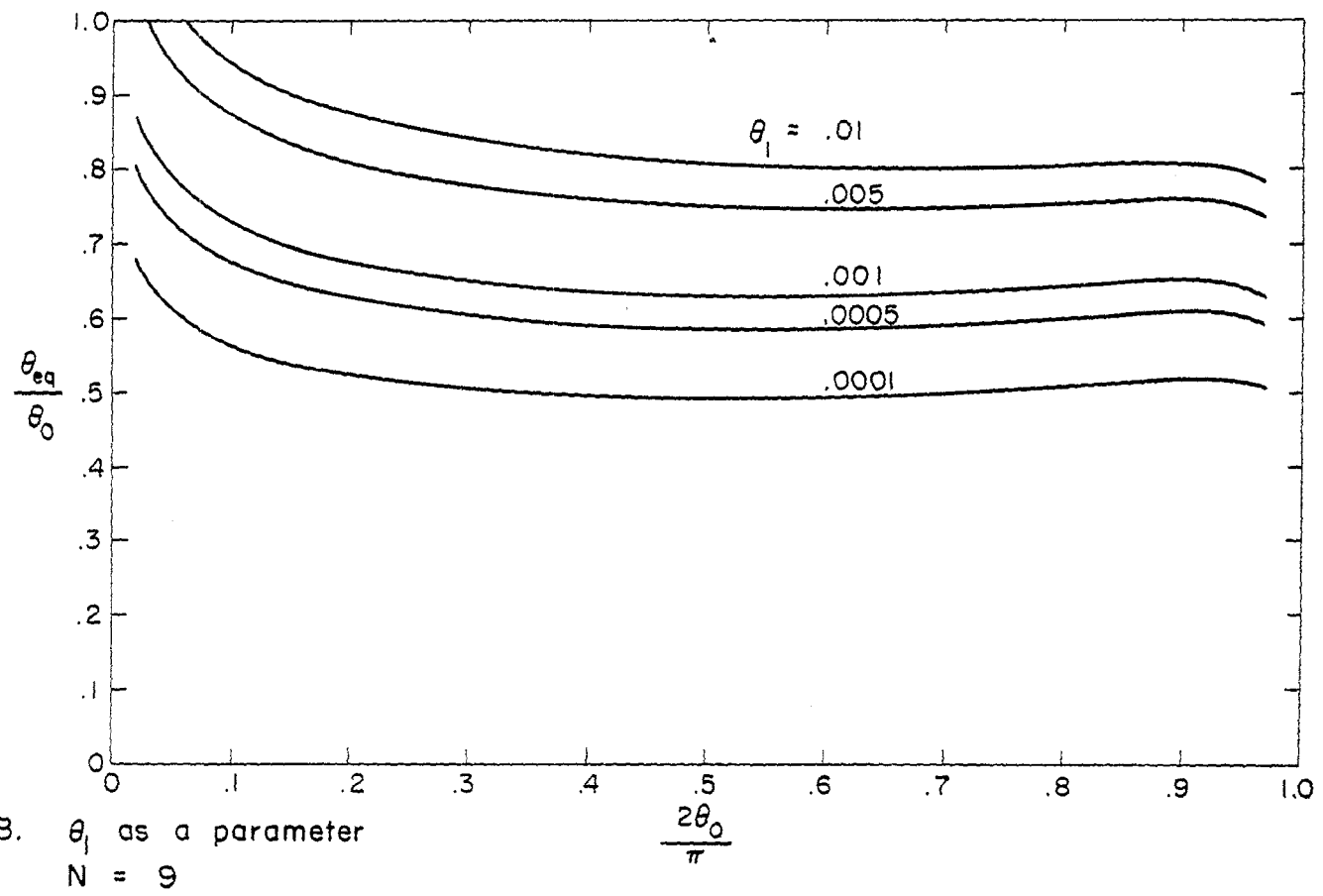
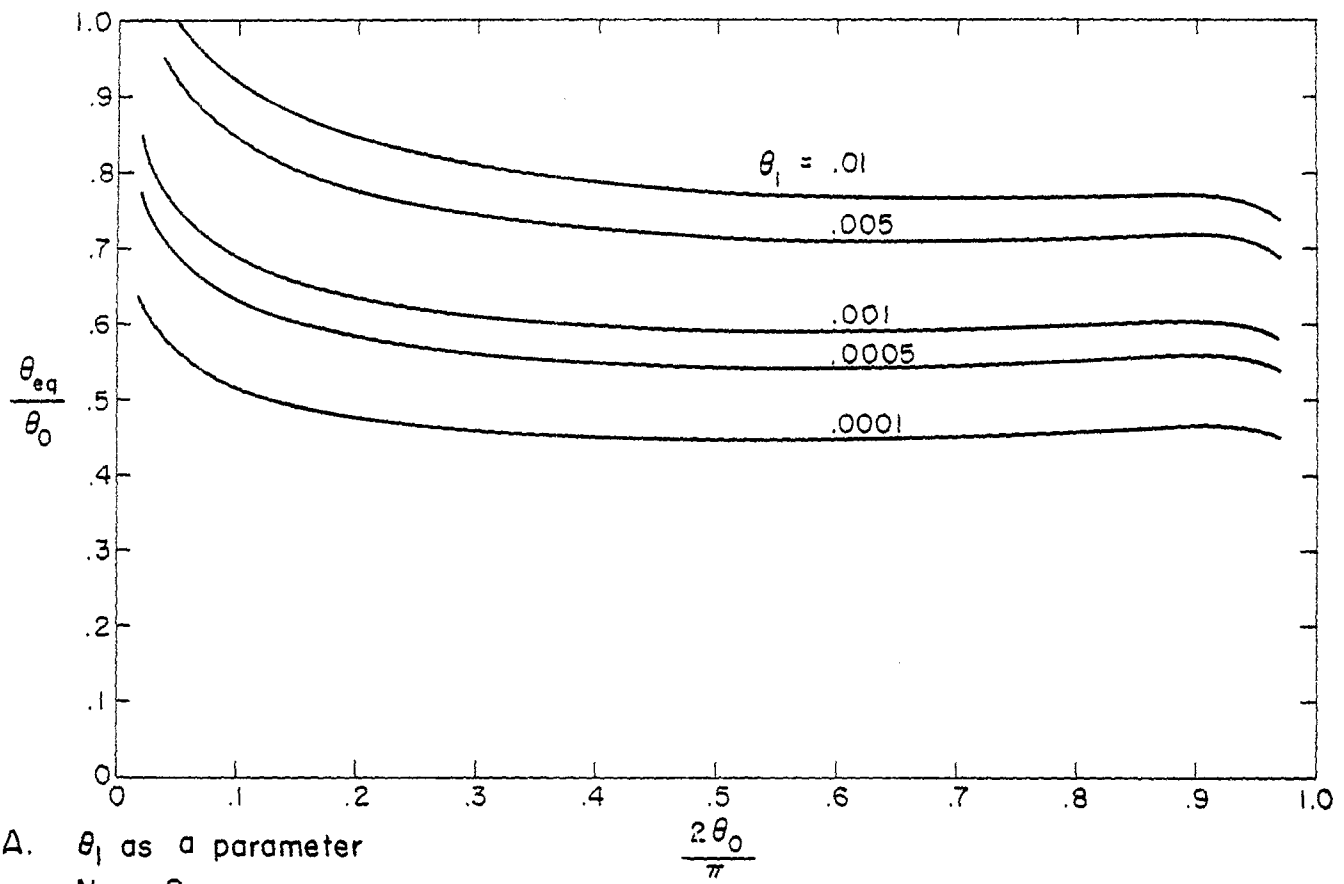


FIGURE 9: EQUIVALENT ANGLE OF A N-WIRE CONE

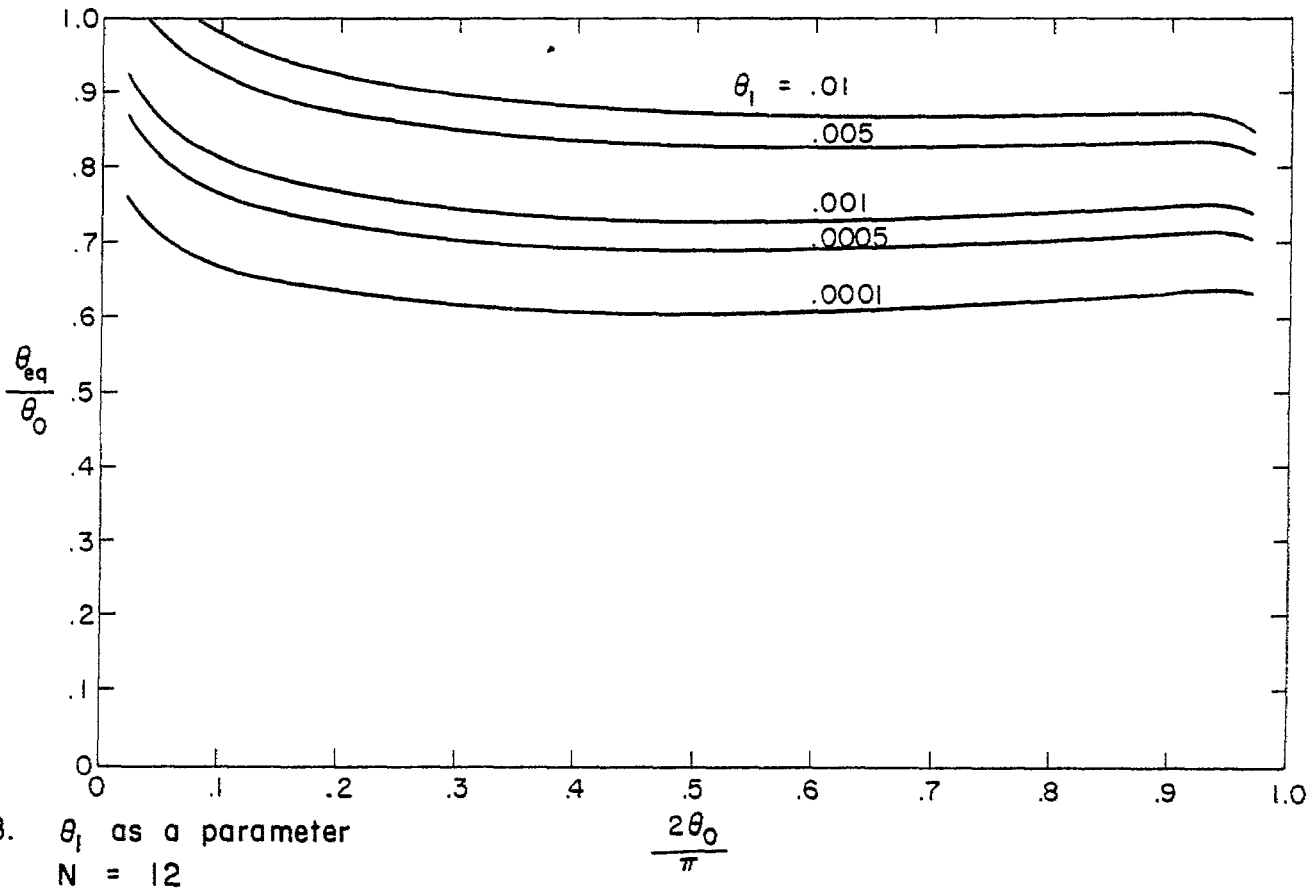
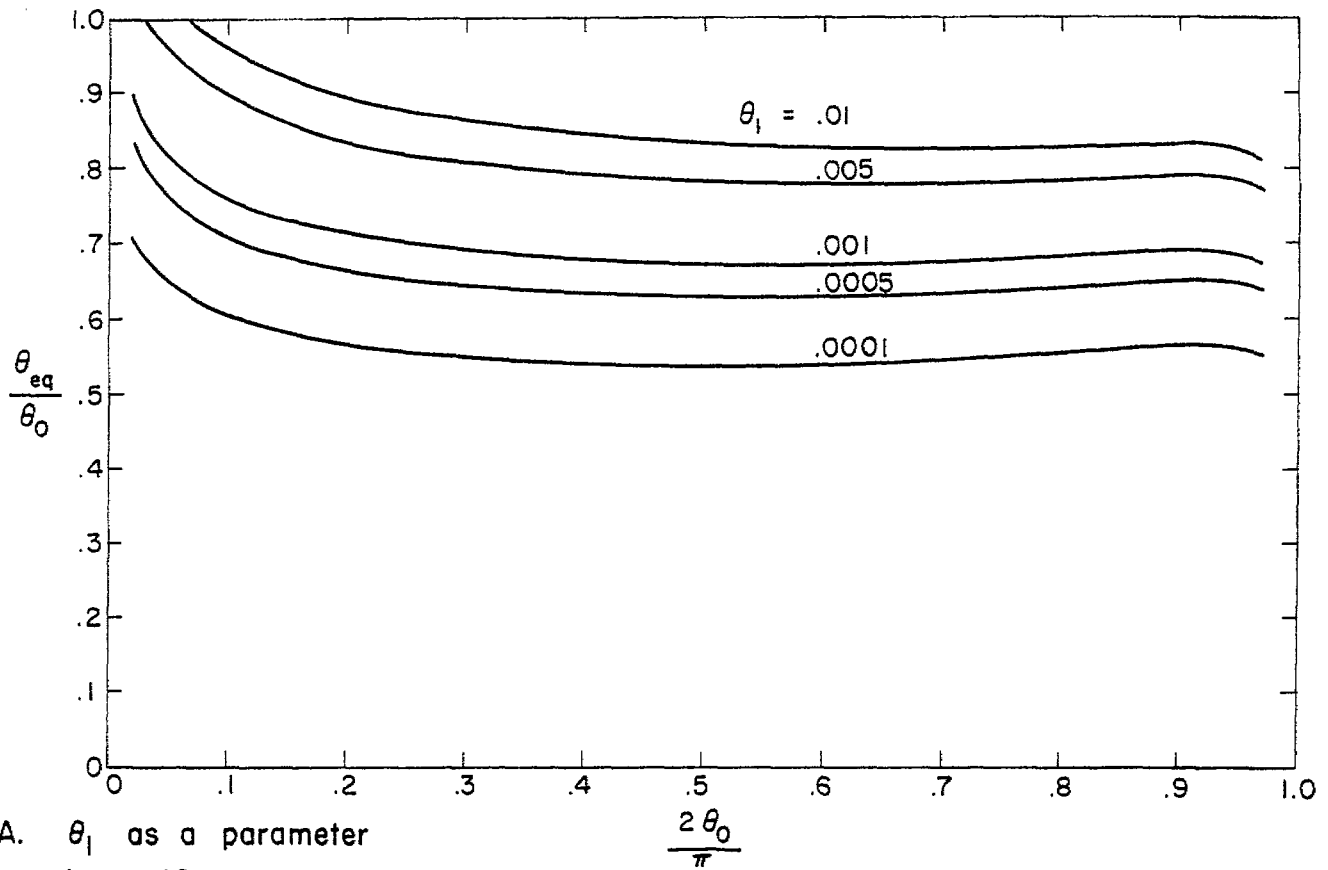


FIGURE 10: EQUIVALENT ANGLE OF A N-WIRE CONE

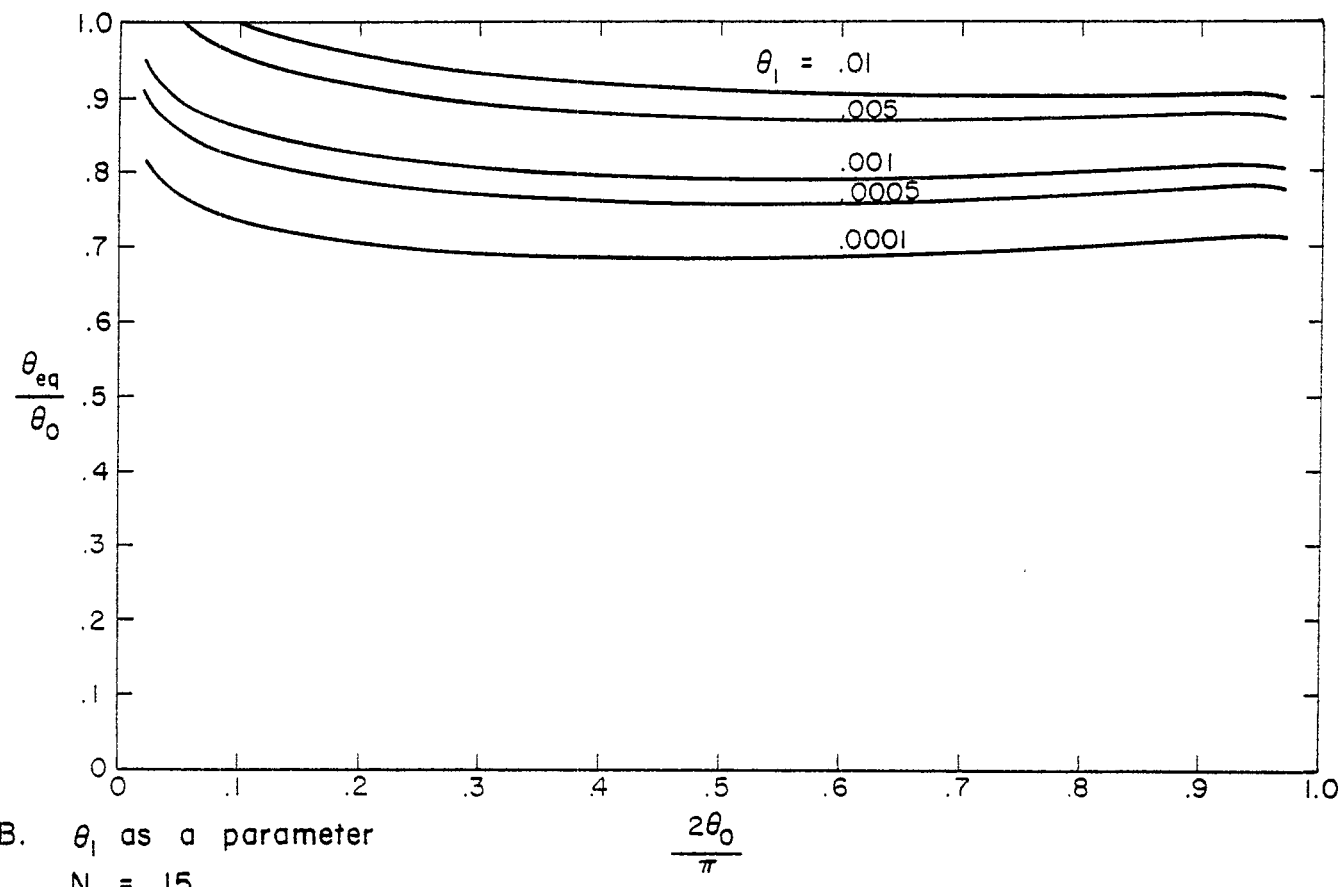
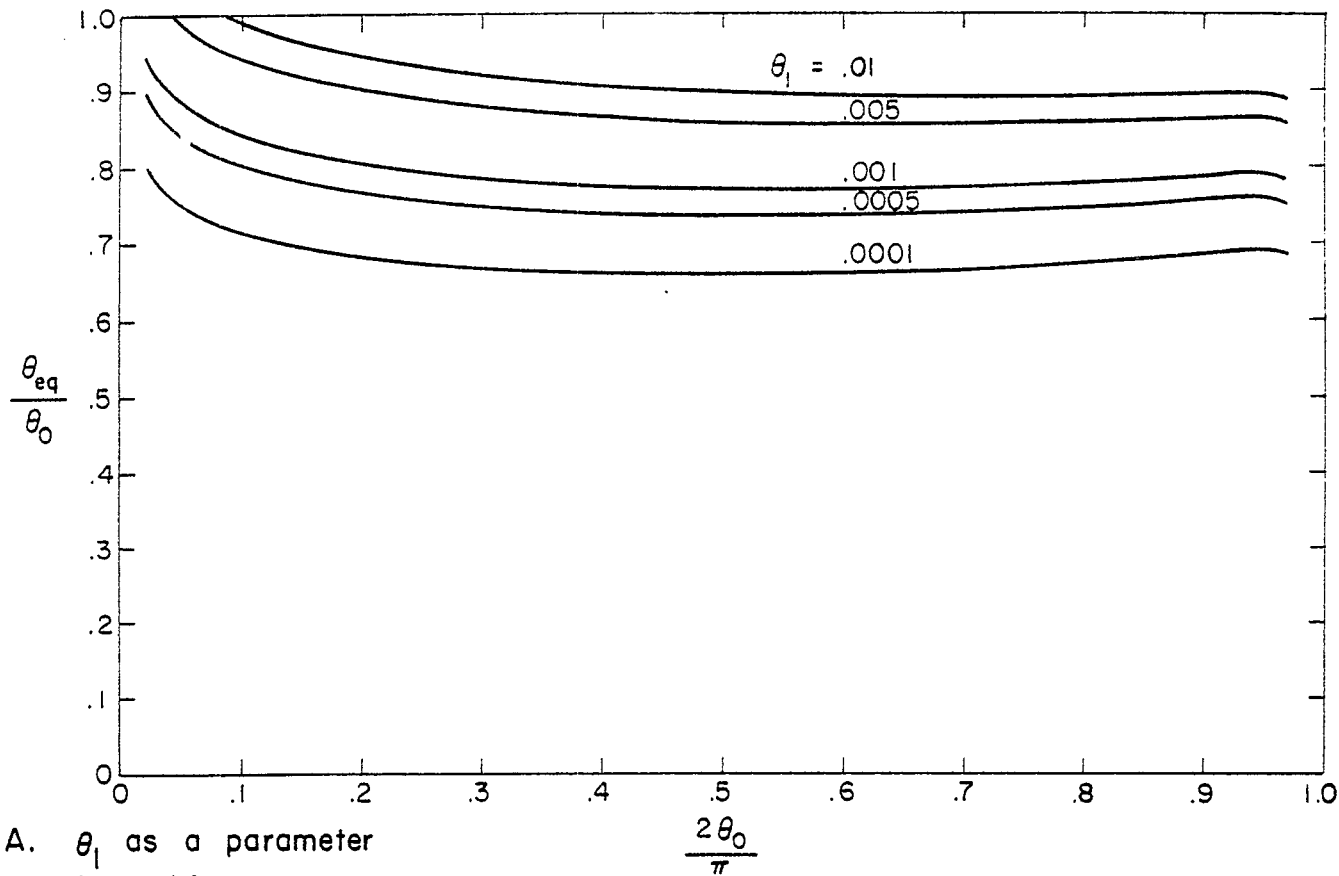


FIGURE 11: EQUIVALENT ANGLE OF A N-WIRE CONE

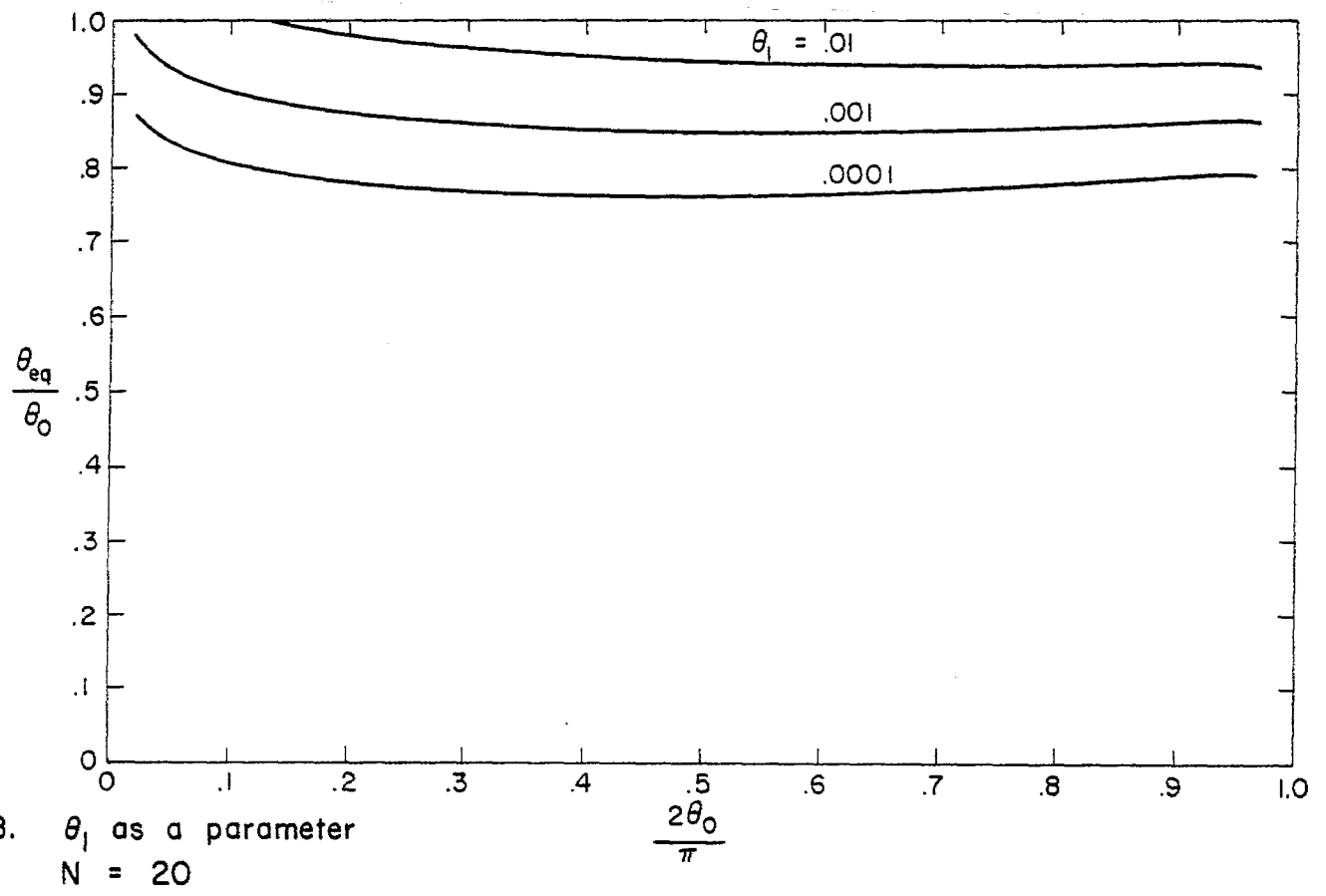
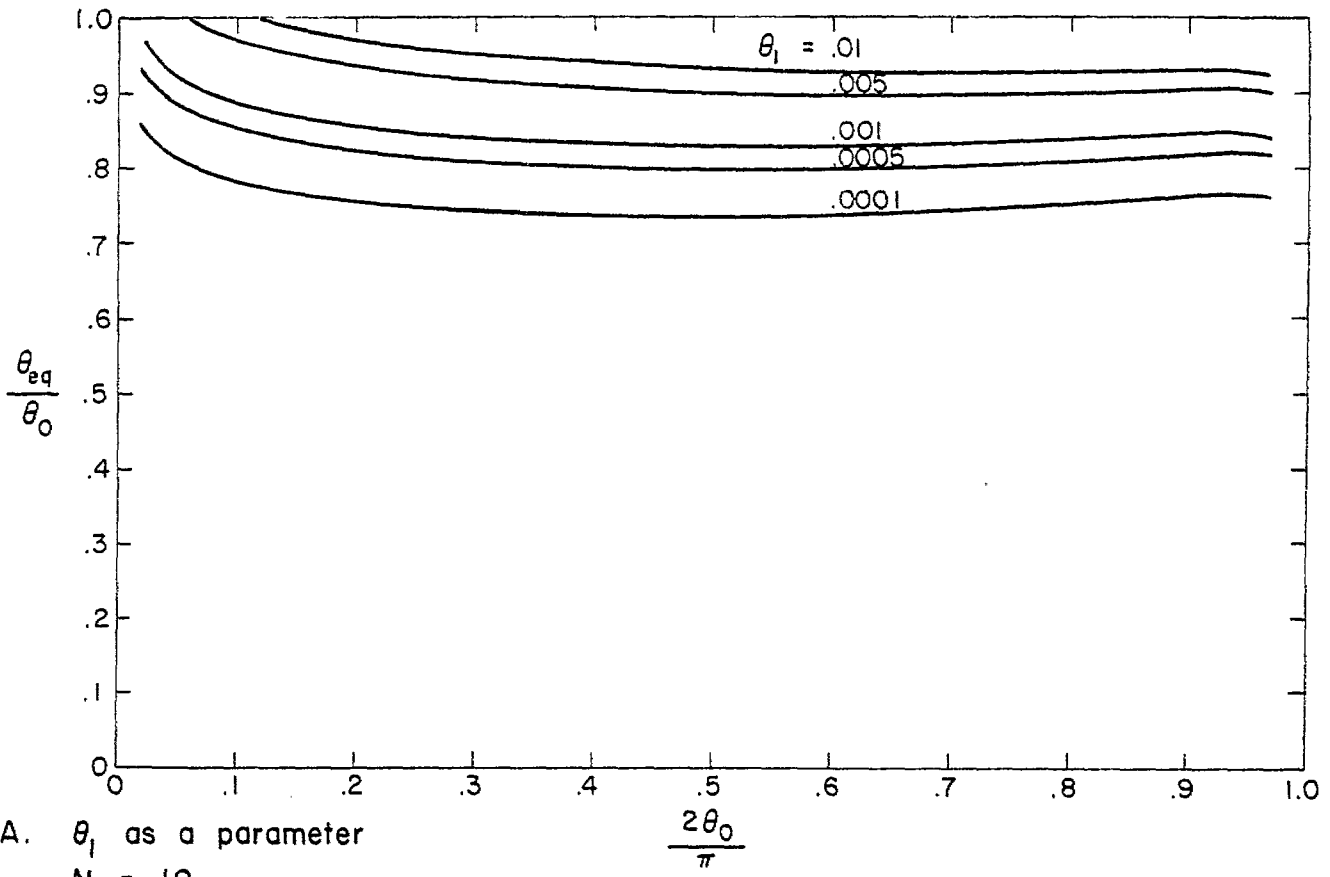


FIGURE 12: EQUIVALENT ANGLE OF A N-WIRE CONE

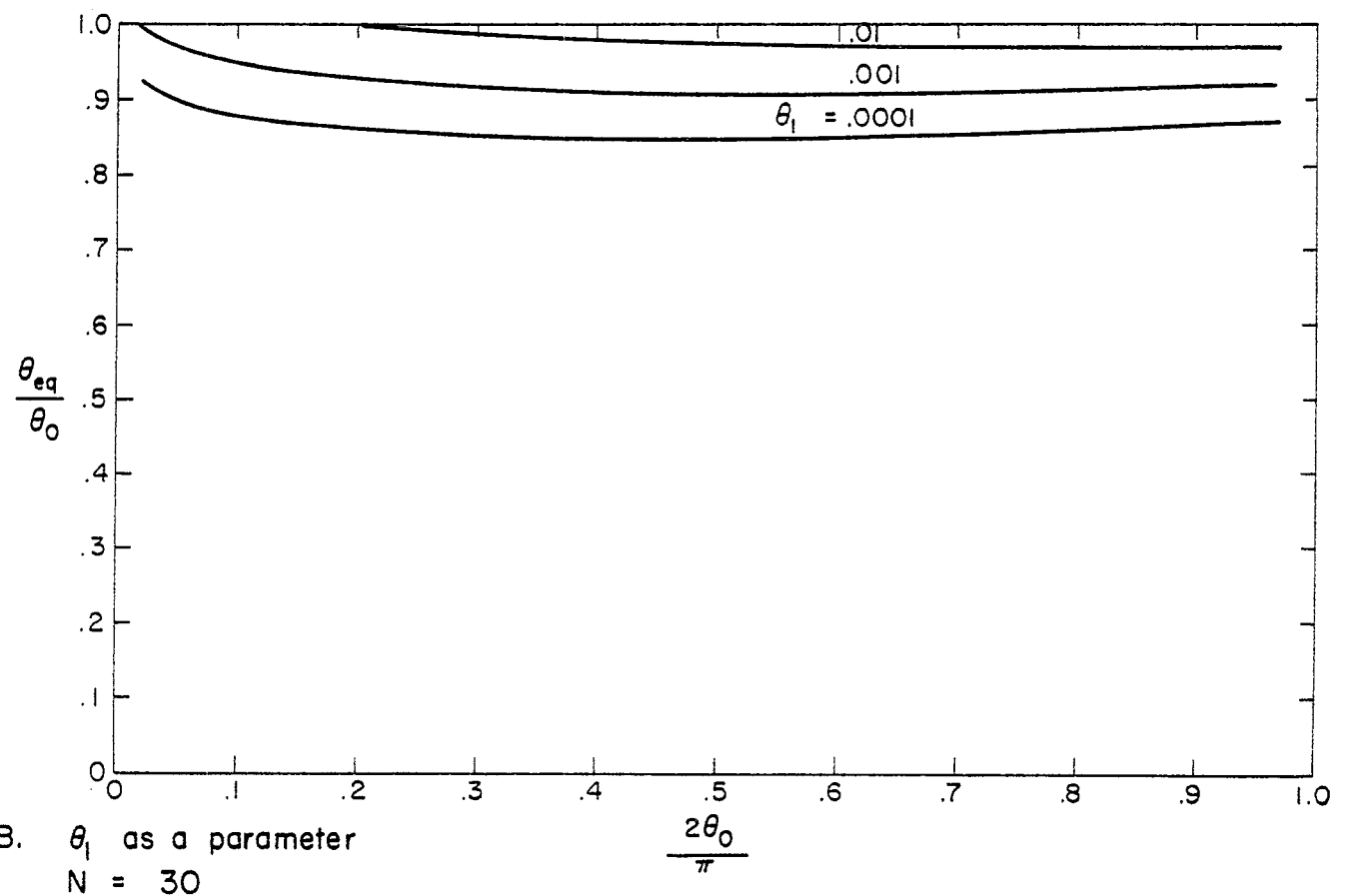
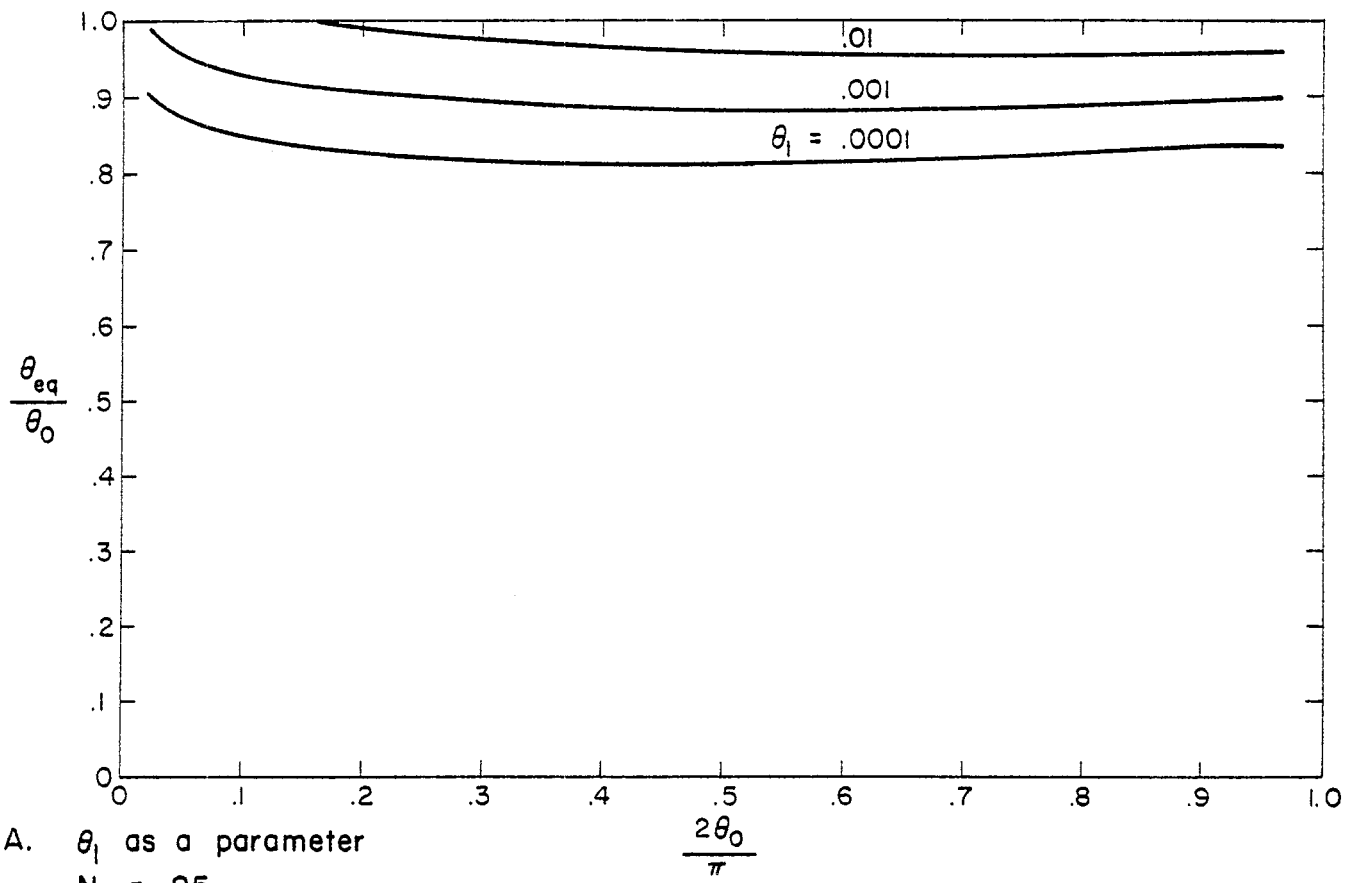


FIGURE 13: EQUIVALENT ANGLE OF A N-WIRE CONE

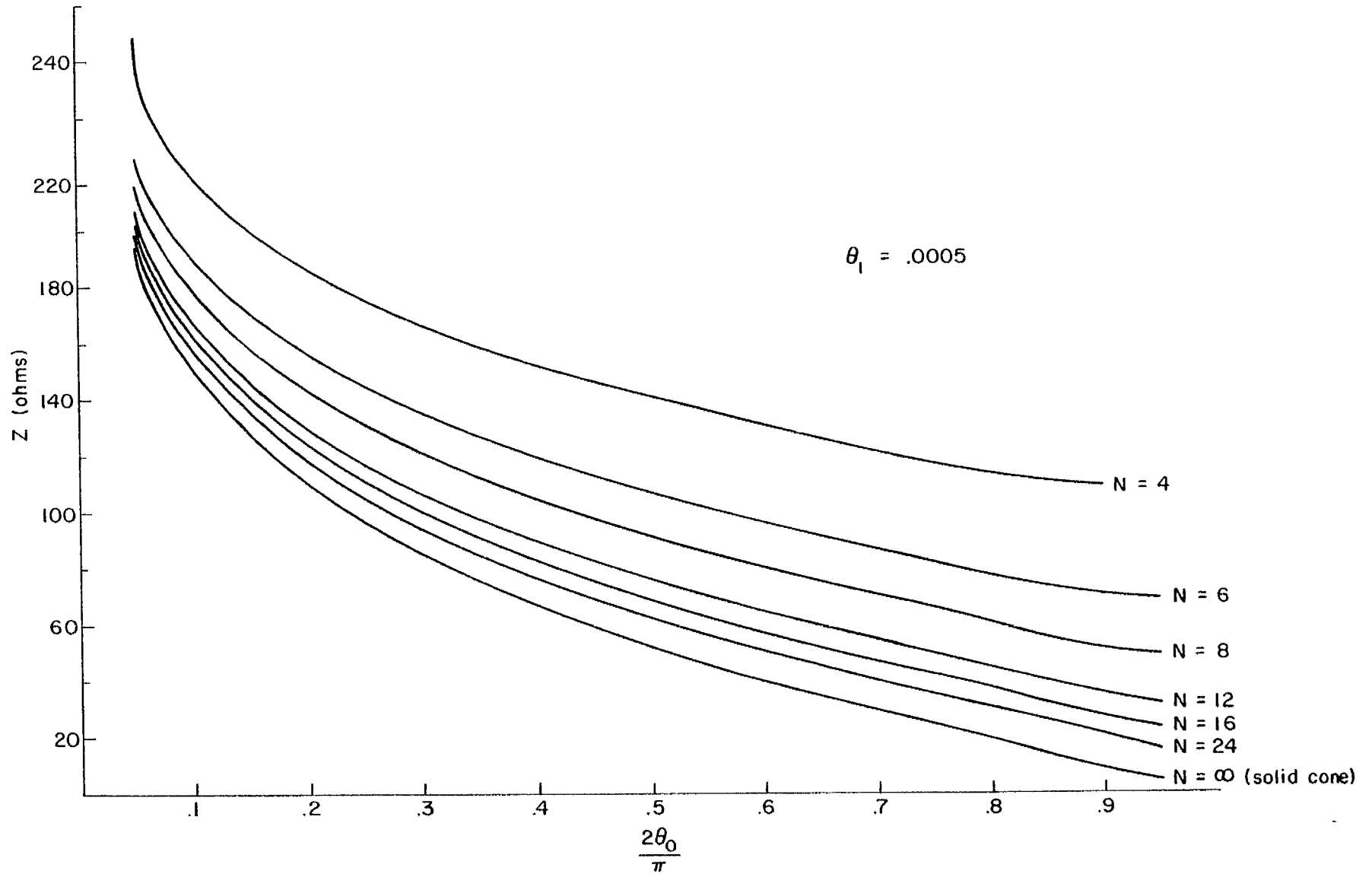


FIGURE 14: IMPEDANCE OF A N-WIRE CONE AS A FUNCTION OF THE HALF ANGLE, θ_0 , FOR $\theta_1 = .0005$

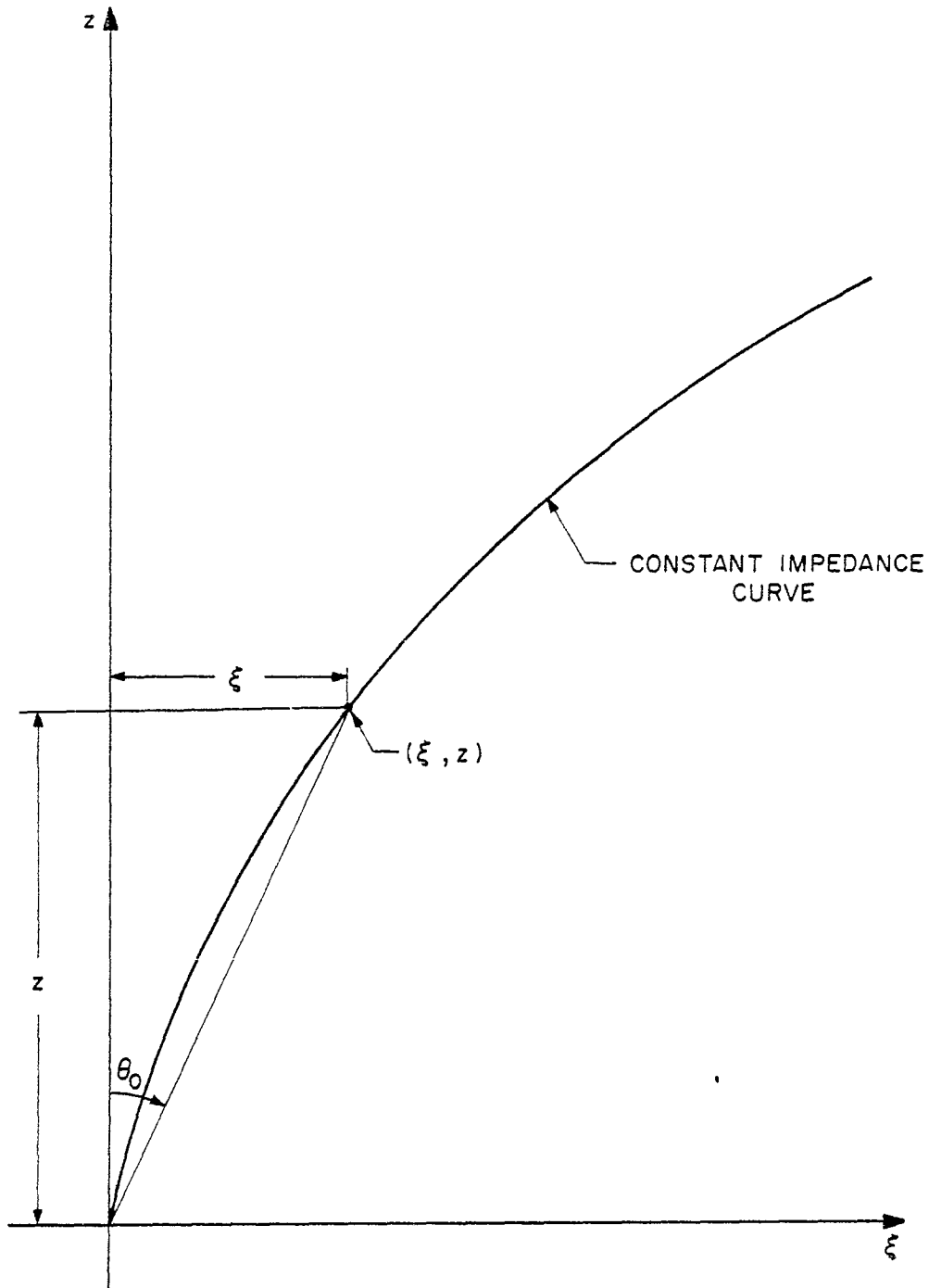
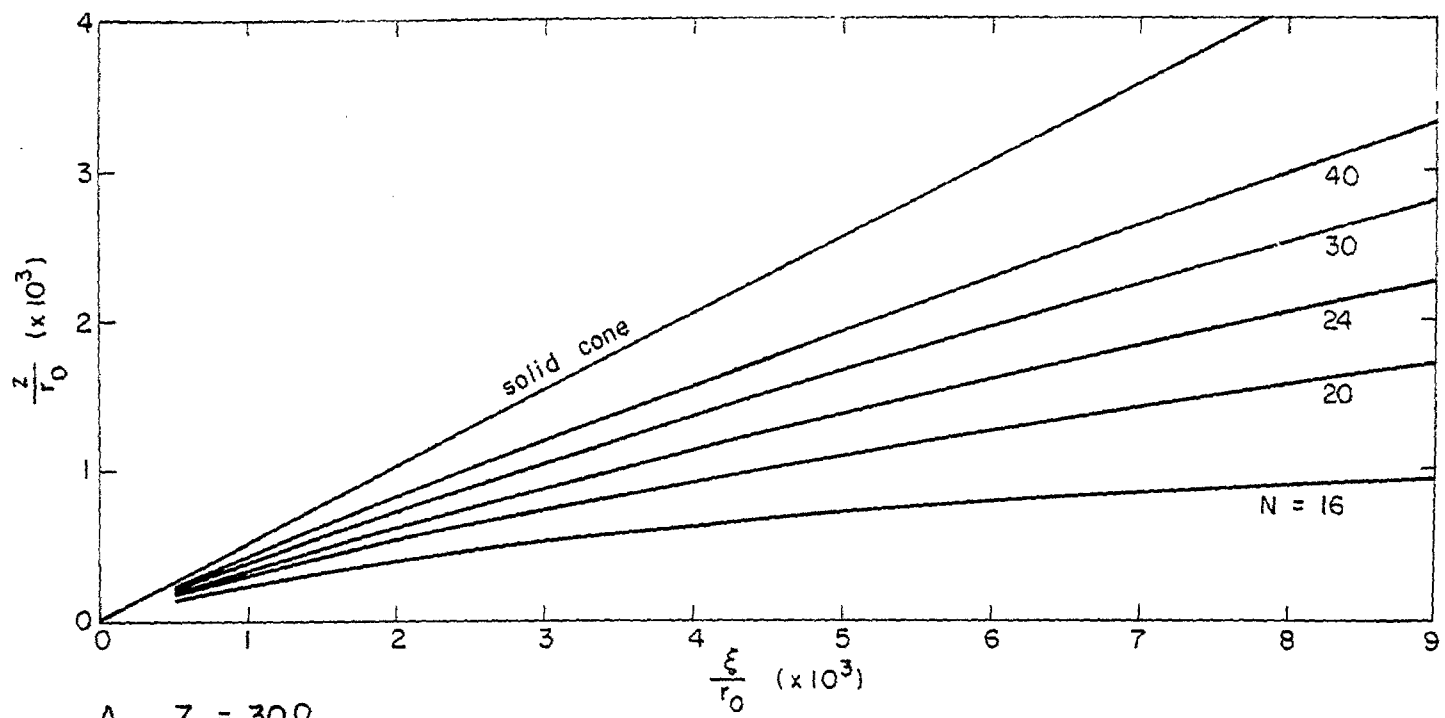
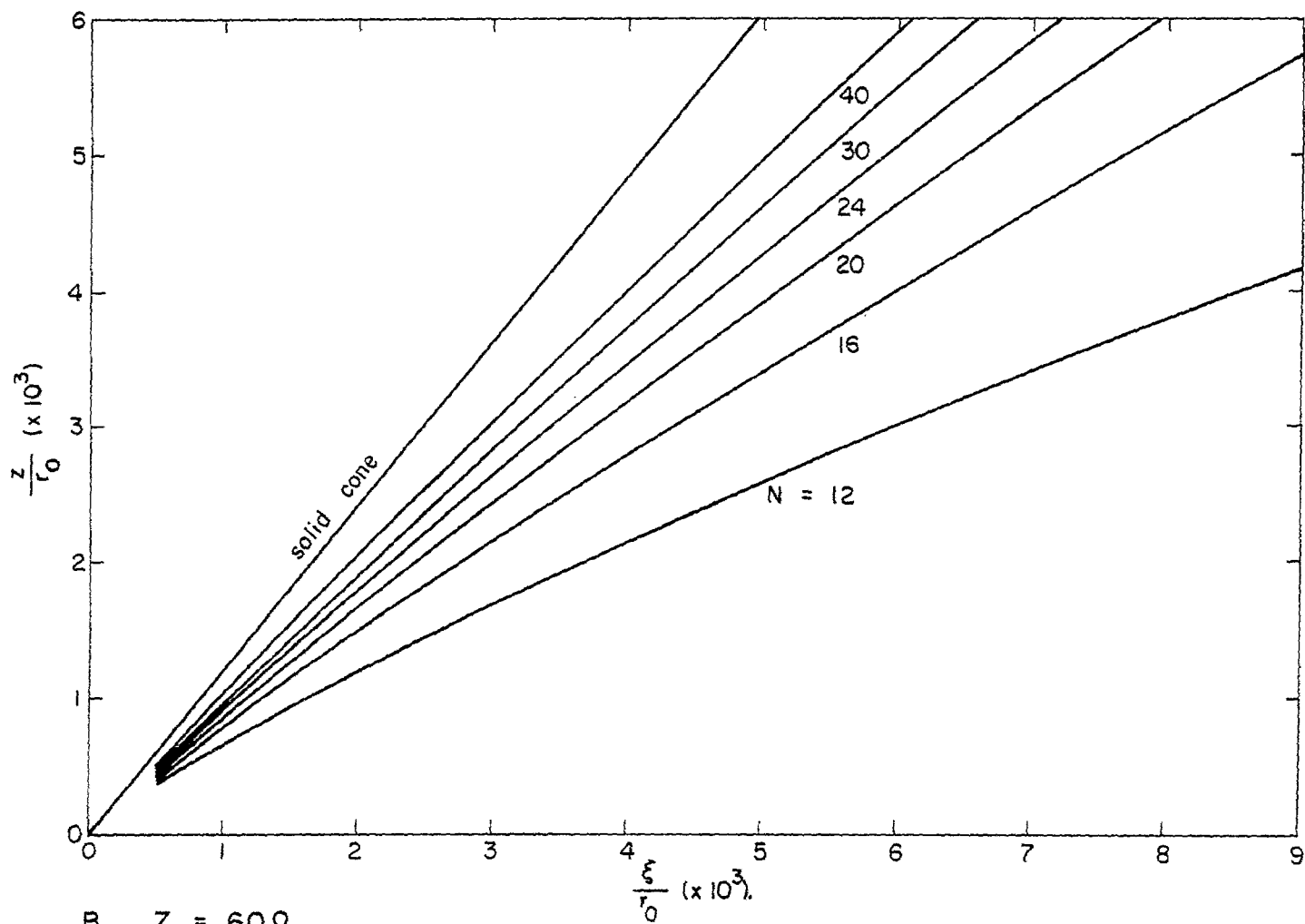


FIGURE 15: CO-ORDINATE SYSTEM OF CONSTANT IMPEDANCE PATH FOR EACH WIRE OF A N-WIRE CONE



A. $Z = 30\Omega$



B. $Z = 60\Omega$

FIGURE 16: CONSTANT IMPEDANCE CURVES FOR N-WIRE CONES

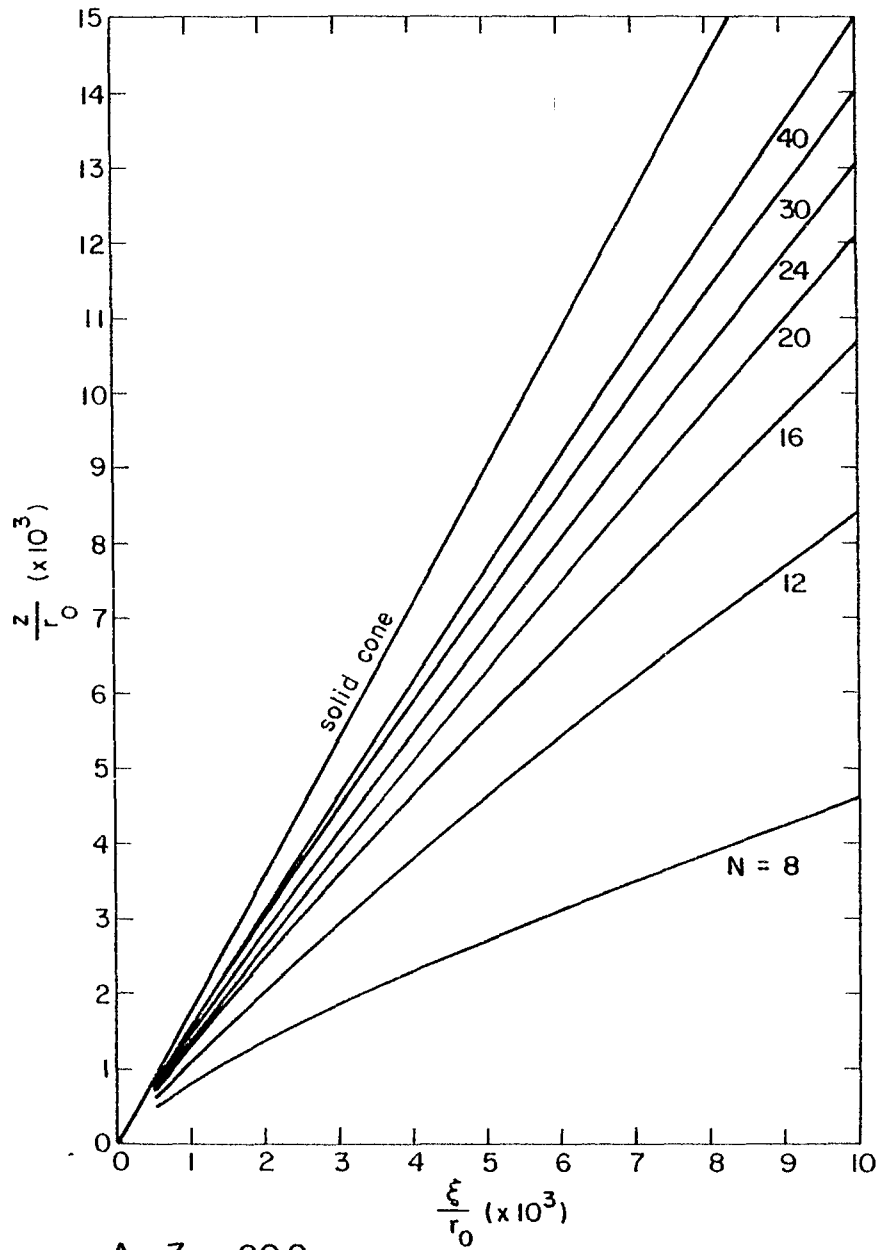
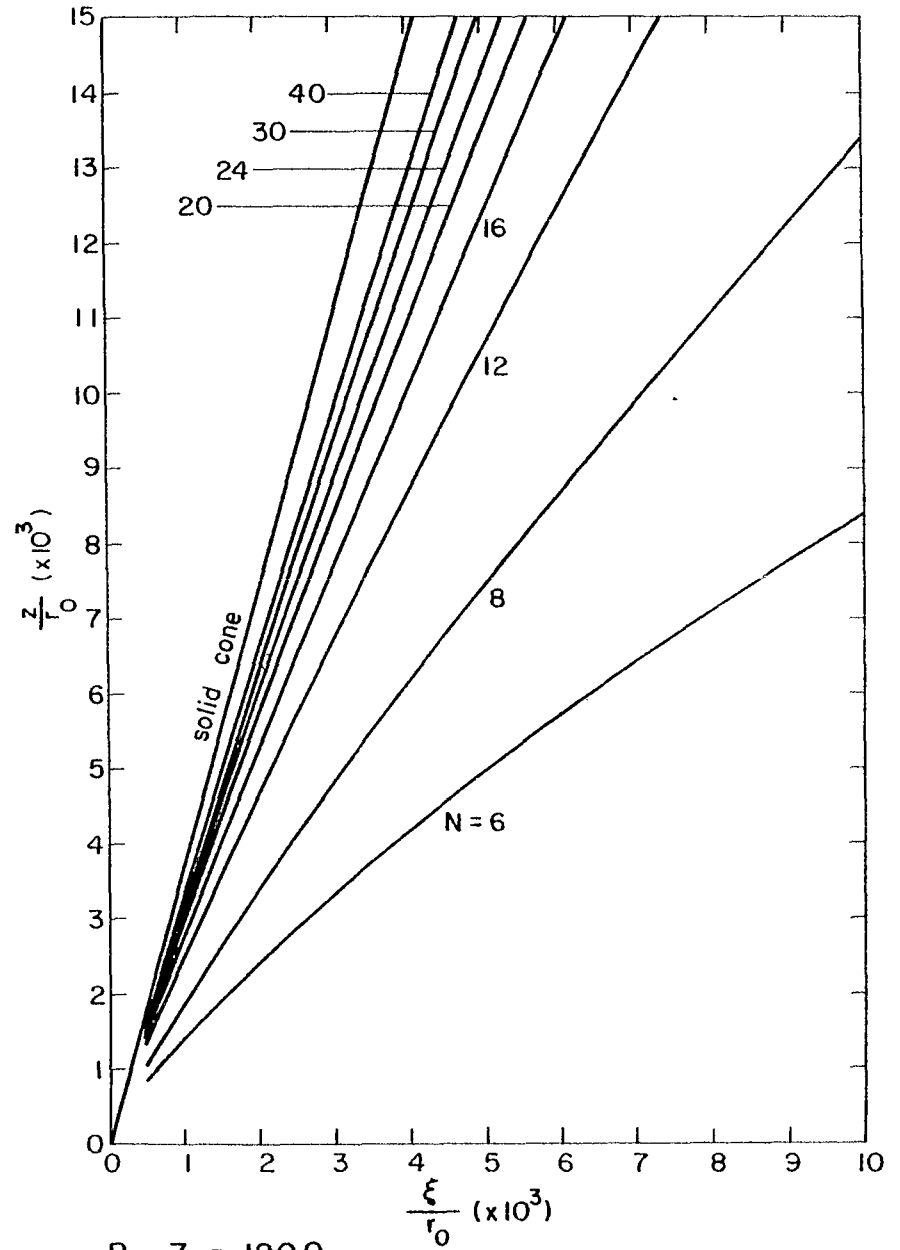
A. $Z = 80\Omega$ B. $Z = 120\Omega$

FIGURE 17: CONSTANT IMPEDANCE CURVES FOR N-WIRE CONES